

**A NOVEL, SINGLE-ISOMER, SULFATED CYCLODEXTRIN FOR USE AS A
CHIRAL RESOLVING AGENT IN CAPILLARY ELECTROPHORESIS: THE
SODIUM SALT OF OCTAKIS(2,3-di-O-methyl-6-O-sulfo)- γ -CYCLODEXTRIN**

A Thesis

by

MICHAEL BRENT BUSBY

Submitted to the Office of Graduate Studies of
Texas A&M University
in partial fulfillment of the requirements for the degree of

MASTER OF SCIENCE

August 2002

Major Subject: Chemistry

**A NOVEL, SINGLE-ISOMER, SULFATED CYCLODEXTRIN FOR USE AS A
CHIRAL RESOLVING AGENT IN CAPILLARY ELECTROPHORESIS: THE
SODIUM SALT OF OCTAKIS(2,3-di-O-methyl-6-O-sulfo)- γ -CYCLODEXTRIN**

A Thesis

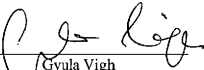
by

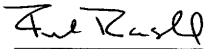
MICHAEL BRENT BUSBY

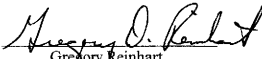
Submitted to the Office of Graduate Studies of
Texas A&M University
in partial fulfillment of the requirements for the degree of

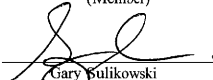
MASTER OF SCIENCE

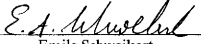
Approved as to style and content by:


Gyula Vigh
(Chair of Committee)


Frank Raushel
(Member)


Gregory Reinhart
(Member)


Gary Sulikowski
(Member)


Emile Schweikert
(Head of Department)

August 2002

Major Subject: Chemistry

ABSTRACT

A Novel, Single-Isomer, Sulfated Cyclodextrin for Use as a Chiral Resolving Agent in
Capillary Electrophoresis: The

Sodium Salt of Octakis(2,3-di-O-methyl-6-O-sulfo)- γ -Cyclodextrin. (August 2002)

Michael Brent Busby, B.S., The University of Texas at Tyler

Chair of Advisory Committee: Dr. Gyula Vigh

A novel, single-isomer, sulfated cyclodextrin, the sodium salt of octakis(2,3-di-O-methyl-6-O-sulfo)cyclomaltooctaose (ODMS) was used as a chiral resolving agent in both aqueous and non-aqueous chiral mediated electrophoretic separation of a large set of pharmaceutically active weak acids and bases as well as UV absorbing neutral enantiomers. Eight of the thirteen weak acids and 45 of the 48 weak bases showed selectivity sufficient for baseline resolution in one or more of the three background electrolytes (BGE's) used. Seven of the sixteen neutral compounds screened were found to exhibit selectivity in at least one of two aqueous BGE's.

A four step synthetic method was used to produce on a large scale the title compound in greater than 98% purity. Synthetic intermediates and the final product were characterized according to purity by HPLC-ELSD and indirect UV-detection capillary electrophoresis (CE), respectively. X-ray crystallography, MALDI-TOF mass spectrometry and ^1H as well as ^{13}C NMR spectroscopy allowed for unambiguous characterization of the structure of each intermediate and the final product.

In memory of my grandmother, Josephine, and to my granddad, Pete.

I won't get his jeans but I hope to fill his shoes.

ACKNOWLEDGEMENTS

Thanks to the Texas Coordination Board of Higher Education TD&T Program for funding this research. Thanks to Steve Silber and Dr. Bob Taylor of the TAMU NMR facility, Dr. Bill Russell of the TAMU Laboratory for Biological Mass Spectrometry, Dr. Joe Reibenspies of the TAMU Crystallography Laboratory and Lisa Thompson from the TAMU Laboratory for Molecular Simulation for their thoughtful contributions.

I would like to thank my research group members including Pavel Glukhovskiy, Dawn Maynard, Alex Sokolowski, Wenhong Zhu, Sanjiv Lalwani, Shulan Li, Ding Li, Kingsley Nzeadibe, Silvia Sanchez-Vindas, Evan Shave and Adriana Salinas. I owe special thanks to members Peniel Lim and Omar Maldonado and of course, my research advisor, Dr. Gyula Vigh.

TABLE OF CONTENTS

	Page
ABSTRACT	iii
DEDICATION	iv
ACKNOWLEDGEMENTS	v
TABLE OF CONTENTS	vi
LIST OF FIGURES	viii
LIST OF TABLES	xi
 CHAPTER	
I INTRODUCTION	1
1.1 Enantiomer Separations by Capillary Electrophoresis.	1
1.2 Cyclodextrins as Charged Chiral Resolving Agents	7
1.3 Single-Isomer Sulfated Cyclodextrins.	13
II SYNTHESIS AND CHARACTERIZATION OF SINGLE-ISOMER ODMS	14
2.1 Synthesis of SiSCD's.	14
2.2 Materials and Methods	17
2.3 Synthesis and Characterization of ODMS and Its Intermediates	19
2.3.1 Octakis(6-O-t-butyltrimethylsilyl)cyclomaltooctaose.	21
2.3.2 Octakis(2,3-di-O-methyl-6-O-t-butyltrimethylsilyl) cyclomaltooctaose.	21
2.3.3 Octakis(2,3-di-O-methyl)cyclomaltooctaose	25
2.3.4 Octakis(2,3-di-O-methyl-6-O-sulfo)cyclomaltooctaose	32
2.4 Discussion of Synthetic Results.	37
2.5 Summary	48
III ENANTIOMER SEPARATIONS.	49

CHAPTER	Page
3.1 Use of ODMS as a Chiral Resolving Agent.	49
3.2 Materials and Methods.	49
3.3 Aqueous Separations	59
3.3.1 Weakly Basic Enantiomer Separations in Aqueous BGE's.	59
3.3.2 Weakly Acidic Enantiomer Separations in Aqueous BGE's.	68
3.3.3 Nonionic Enantiomer Separations in Aqueous BGE's.	73
3.4 Weakly Basic Enantiomer Separations in Methanolic BGE's.	83
3.5 Summary.	91
IV CONCLUSIONS.	92
REFERENCES	95
APPENDIX A: LETTERS OF COPYRIGHT CREDIT	99
APPENDIX B: EXPERIMENTAL	102
VITA	115

LIST OF FIGURES

FIGURE		Page
1	Peak resolution surfaces for 7-charged and 14-charged analytes as a function of separation selectivity and normalized electroosmotic mobility.	6
2	Spacefill rendering of the crystal structure of native γ -cyclodextrin shown in (A) annular view and (B) side-on view.	8
3	Illustration of the potential substitution patterns observable in the functionalization of the primary hydroxyl groups of native γ -cyclodextrin. . .	15
4	Synthetic scheme for octakis(2,3-di-O-methyl-6-O-sulfo) cyclomaltooctaose.	20
5	^1H -NMR spectrum of (2) in CDCl_3	22
6	A section of the MALDI-TOF mass spectrum of (2).	23
7	Crystal structure of (2).	24
8	Assigned ^1H and ^{13}C -NMR of (3) in CDCl_3	26
9	A section of MALDI-TOF mass spectrum of (3).	27
10	Crystal structure of (3).	28
11	Assigned ^1H and ^{13}C -NMR of (4) in D_2O	29
12	A section of the MALDI-TOF mass spectrum of (4).	30
13	Crystal structure of (4).	31
14	Indirect UV-detection CE of recrystallized (5).	33
15	Assigned ^1H and ^{13}C -NMR of (5) in D_2O	34
16	A section of the MALDI-TOF mass spectrum of (5).	35
17	Crystal structure (A) and Connolly solvent surface (B) of (5).	36

FIGURE	Page
18 ELSD traces of (1) (A) prior to recrystallization and (B) after recrystallization.	38
19 Horvath plot of components of a sample obtained by mixing acetone/methanol mixed mother liquors	39
20 Comparison of ¹ H-NMR spectra of (2) (A) with known over-silylation impurity and (B) of a previously well characterized 14-silylated β-CD.	41
21 ELSD traces for the optimization of the methylation of (2)	42
22 Evaluation of the suitability of indirect UV-detection CE for use in monitoring the sulfation of (4).	44
23 DQ-COSY spectrum of (5) in D ₂ O	46
24 HETCOR spectrum of (5) in D ₂ O	47
25 Names and structures of weak acid analytes	50
26 Names and structures of weak base analytes	51
27 Names and structures of non-ionic analytes.	53
28 Injection sequence for sandwich method.	56
29 Sandwich method overlays.	57
30 Mobility a) and separation selectivity b) curves for B33 (+), B14 (×) and B45 (⊗) in pH 2.5 aqueous BGE	62
31 Capillary electrophoretic separations of some weakly-binding bases using ODMS as chiral resolving agent in pH 2.5 aqueous BGE	63
32 Mobility a) and separation selectivity b) curves for B18 (+), B38 (×) and B42 (⊗) in pH 2.5 aqueous BGE.	66
33 Capillary electrophoretic separations of some strongly-binding bases using ODMS as chiral resolving agent in pH 2.5 aqueous BGE	67

FIGURE	Page
34	Capillary electrophoretic separations of some weakly basic analytes using ODMS as chiral resolving agent in pH 9.5 aqueous BGE 69
35	Mobility a) and separation selectivity b) curves for A02 (+), A22 (×) and A31 (⊗) in pH 2.5 aqueous BGE 71
36	Capillary electrophoretic separations of weakly acidic analytes using ODMS as chiral resolving agent in pH 2.5 aqueous BGE 72
37	Capillary electrophoretic separations of non-ionic analytes using ODMS as chiral resolving agent in pH 2.5 aqueous BGE 73
38	Mobility a) and separation selectivity b) curves for B42 (+), B14 (×) and B49 (⊗) in acidic methanol BGE 84
39	Capillary electrophoretic separations of weakly basic analytes using ODMS as chiral resolving agent in acidic methanol BGE 86

LIST OF TABLES

TABLE		Page
1	Electrophoretic data for weakly basic, acidic and non-ionic analytes in pH 2.5 aqueous BGE	75
2	Electrophoretic data for weakly basic, acidic and non-ionic analytes in pH 9.5 aqueous BGE	79
3	Electrophoretic data for weakly basic analytes in acidic methanol BGE.	88

CHAPTER I

INTRODUCTION

1.1 Enantiomer Separations by Capillary Electrophoresis

A chiral molecule is one that is non-superimposable on its mirror image. For a molecule to be chiral, it must not possess any second-order symmetry element including a mirror plane, an inversion center or a rotation-reflection axis. Two chiral molecules that possess identical atomic constitution but differ in the three dimensional arrangement of their atoms are stereoisomers of one another. Examples of stereoisomers include, but are not limited to diastereomers and enantiomers. While diastereomers are stereoisomers, they are not mirror images of one another and thus, they are often sufficiently different in some physical property that will facilitate their separation. Enantiomers, however, are stereoisomers that are also mirror images of one another. Enantiomeric species have all similar physical properties except that they rotate plane polarized light with the same magnitude in opposite directions. For this reason, they are often referred to as optical isomers.

Separation of enantiomeric molecules has long been attractive to researchers not only for reasons of academic interest but also because they are ubiquitous in living systems. Chirality plays a fundamental role in the processes of living systems where stereoisomers are almost always distinguishable in their pharmacokinetic and toxicologic effects. A prime example is thalidomide, introduced in 1954 as a muscle relaxant for

This thesis follows the style and format of Journal of Chromatography A.

pregnant women. It was sold as a racemic mixture of both optical isomers. While one isomer functioned solely as an effective muscle relaxant, the other was unknowingly a teratogen. The ingestion of the racemate by the pregnant mothers resulted in thousands of children being born with severe birth defects. Awareness of the role of chirality in living systems eventually prompted the FDA to adopt policies requiring qualitative and quantitative knowledge of the isomeric composition of any drug brought to clinical trials and that manufacturing specifications include, “assurance of identity, strength, quality and purity” of the composition from a stereochemical viewpoint [1].

Research in chiral resolution and more specifically enantiomer resolution has since exploded. Developments in asymmetric synthesis and combinatorial chemistry have led to demand for high speed, high throughput analysis using minute sample amounts and inexpensive materials. Analytical separation methods commonly used for enantioseparation include thin layer chromatography (TLC) [2], gas chromatography (GC) [3], high performance liquid chromatography (HPLC) [4], capillary electrochromatography (CEC) [5] and micellar electrokinetic chromatography (MEKC) [6], all of which use chiral modified stationary and/or mobile phases to bring about the separation of chiral analytes. Free zone capillary electrophoresis (FZCE) has become increasingly popular due to its inherent high efficiency, inexpensive material requirements and ease of automation. Each of the aforementioned analytical techniques suffers to different degrees from multiple band broadening mechanisms. TLC, HPLC and MEKC are inherently lower efficiency separation methods than FZCE, with HPLC and MEKC providing only around 20,000 theoretical plates/column due, predominantly, to band broadening effects

related to resistance to mass transfer and, in the case of MEKC, electromigration dispersion (EMD) effects. TLC is 1 to 3 orders of magnitude lower in separation efficiency. Open tubular GC, although limited to analysis of samples with volatile components, offers around 100,000 theoretical plates/column and is probably the most versatile chiral analysis tool with current commercially available instruments equipped with both universal and specific detectors and well over 100 different chiral stationary phases available. FZCE is limited to the analysis of ionic samples soluble in some electrically conductive solvent, but offers higher separation efficiency than any other separation method. Because there is no stationary phase, FZCE suffers only diffusive band broadening and EMD, with separation efficiencies often exceeding 1,000,000 theoretical plates/column. Detection methods most commonly used in CE are UV detection however, the development of suitable detection methods for use with capillary electrophoresis is ongoing. Many recent advancements have been made including coupling CE to various mass spectrometric detectors [7-9], NMR [10], near-IR/Fluorescence [11] and, most recently, nitrogen specific chemiluminescence detectors [12].

CE separations are based on the difference in the charge to hydrodynamic radius ratio of the sample components in the BGE under an applied electric field. This relation is expressed by Stokes' mobility (μ^{theor}) equation,

$$\mu^{\text{theor}} = ze_0 / 6\pi\eta a \quad (1)$$

where z is the component charge, e_0 is the elementary charge, η is the molecular viscosity and a is the hydrodynamic radius of the migrating component. This relation has

only limited applicability as it is difficult to obtain exact and meaningful values for either the molecular viscosity or the hydrodynamic radius experienced by a migrating ion [13]. Mobility relates the speed (s) with which each component moves through the applied field to the applied field strength (E^{app}). The constant of proportionality is a component's observed mobility (μ^{obs}),

$$s = \mu^{obs} E^{app} \quad (2)$$

which is a function of the migrating components effective mobility and the nonspecific electroosmotic mobility (μ^{eo}).

$$\mu^{obs} = \mu^{eff} + \mu^{eo} \quad (3)$$

The electroosmotic flow (EOF) is an electrohydrodynamic phenomenon. The EOF in a capillary has a plug-like flow profile and thus causes little band broadening.

Electroosmotic mobility is related to the zeta potential (ζ),

$$\mu^{eo} = \frac{\zeta \epsilon}{\eta} \quad (4)$$

where ϵ is the relative permittivity of the BGE. The EOF can be controlled by fixing either the zeta potential or the viscosity of the BGE. Control of the zeta potential can be as simple as buffering the pH of the BGE [14].

The acidic silanol groups formed from hydrolysis of the wall of fused silica capillaries have pKa's in the range of 1.5 to 7.0. At low pH, the EOF is maintained at relatively low values because the charge density of the capillary wall is low as compared to that observed at high pH where more of the silanol groups are deprotonated. Other means to control the EOF include capillary wall coating and covalent modification of the

capillary wall.

In CE, peak resolution is not dictated by separation selectivity alone but, is also dependent on the relative migration direction and magnitude of the mobility of the enantiomers and the EO. Normalized electroosmotic mobility (β) is defined as,

$$\beta = \mu^{\text{eo}}/\mu_2^{\text{eff}} \quad (5)$$

where μ_2^{eff} is the effective mobility of the slower enantiomer. When $\beta = -1$, the EOF is equal in magnitude but opposite in direction to the mobility of the more slowly migrating species. The result is the more slowly migrating enantiomer is locked in its position in the capillary while the other enantiomer migrates away from it. Rawjee and Vigh [15] proposed a resolution (R_s) equation for CE that takes into account the effects of the β value.

$$R_s = \sqrt{\frac{E l \epsilon_0}{8 k t}} \frac{(|\alpha - 1|)\sqrt{|\alpha + \beta|} \sqrt{z_1^{\text{eff}}} \sqrt{z_2^{\text{eff}}}}{\sqrt{|\alpha + \beta|^3 ||z_1^{\text{eff}}| + \sqrt{|\alpha|(1 + \beta)^3 ||z_2^{\text{eff}}|}} \quad (6)$$

where l is the capillary length, k is Boltzman's constant and α is the separation selectivity defined as $\alpha = \mu_1^{\text{eff}}/\mu_2^{\text{eff}}$. For CE enantiomer separations, the convention is to assign subscript 2 to the enantiomer, either R or S, that migrates more slowly at the lowest chiral selector concentration used. This definition yields separation selectivity values in the $-\infty < \alpha < \infty$ range. The resolution surfaces generated from equation 6 and shown in figure 1 illustrate that resolution in CE can be improved with use of higher electric potentials, controlling the EOF to keep β near -1, increasing separation selectivity and through increase of the effective charge of the enantiomers.

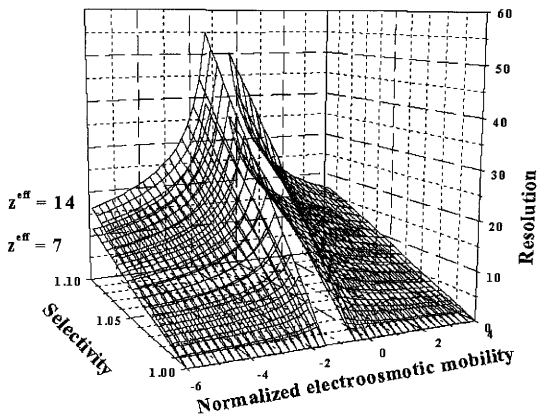


Figure 1. Peak resolution surfaces for 7-charged and 14-charged analytes as a function of separation selectivity and normalized electroosmotic mobility.

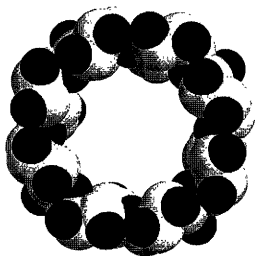
1.2 Cyclodextrins as Charged Chiral Resolving Agents

Separation of enantiomers involves their differentiation through diastereomeric interaction with other optically active molecules. While many different chiral resolving agents have been investigated for use in enantiomer separations including but not limited to chiral crown ethers [16], chiral cryptands [17], proteins, chiral surfactants and macrocyclic antibiotics [18], cyclodextrins (CD's) have moved to the forefront of enantiomer separations research [19-22]. This is in part because native CD's are inexpensive and frequently form stable inclusion complexes with both small and large molecules alike. Also, CD's are versatile chiral selectors since they are easily derivatized to yield changes in their selectivity for different separation applications.

Cyclodextrins are toroidal shaped molecules capable of host-guest interactions. A cavity formed by α (1-4) cyclization of amylose allows for inclusion of guest molecules. CD's are naturally occurring species produced by the enzymatic degradation of starch by cyclodextrin glucosyl transferases (CGTases) industrially harvested from bacillus macerans and used to produce α -, β - and γ -CD's with 6, 7 and 8 D-glucopyranoside units [23], respectively. Figure 2 shows the crystal structure of native γ -CD. The chiral environment within and about the cyclodextrin cavity provides the molecular recognition mechanism required for stereodifferentiation of enantiomers and makes their separation possible.

Neutral cyclodextrins used for CE enantiomer separations include the native species as well as those modified with neutral functionalities, most commonly methyl, acetyl and hydroxypropyl. Per- substitution of native cyclodextrin can yield an isomer

A



B

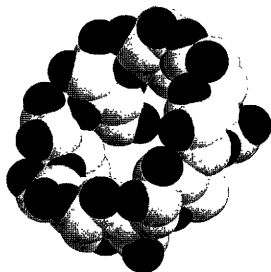


Figure 2. Spacefill rendering of the crystal structure of native γ -cyclodextrin shown in (A) annular view (B) side-on view. Oxygen atoms are dark and carbons atoms are light. Hydrogen atoms are omitted for clarity.

species with modification of all available substitution sites. Their use is reliable and reproducible since there is only a single cyclodextrin species present in the BGE [24-25]. However, neutral cyclodextrins are often poorly soluble in common solvents used for BGE's. For example, the solubility of native α -, β - and γ -CD's in aqueous BGE's is 0.12, 0.016, and 0.17 M, respectively[26].

It is interesting to note that while β -CD is the preferred native CD for use in CE enantiomer separations because of its greater availability, it is by far the least soluble native CD. The relative poor solubility of β -CD as compared to other native CD's is in part due to the extensive hydrogen bonding network of its secondary hydroxyl rim resulting in more disfavorable enthalpy and entropy of dissolution [27]. Substitution of the secondary rim of native CD's has been shown to actually increase the solubility in aqueous BGE's presumably because substitution breaks the hydrogen bonding network. The most notable is a thirty-fold greater solubility of (2,6-di-O-methyl) β -CD than its native counterpart [28].

A wide variety of derivatized CD's are now available and have been used successfully for enantiomer resolution by CE. Often, the observed selectivity can be modified according to experimental need simply by changing the CD in the BGE [29-31]. However, neutral CD's are limited in application to the separation of charged enantiomers as they are not able to impart charge to neutral ones. This limitation has led to interest in charged cyclodextrins for the CE separation of neutral compounds.

Charged cyclodextrins offer the ability to separate neutral species [32-33]. Complexation of neutral enantiomers with charged CD's results in charged complexes

that have the potential to be separated based on the difference in their charge to size ratio. Currently, both weak electrolyte [34-35] and strong electrolyte [36-38] charged CD's are used. Both types have their advantages and disadvantages in use [39]. Strong electrolyte CD's are charged over the entire pH range while weak electrolyte CD's are charged at only high or low pH's.

Strong electrolyte cyclodextrins are functionalized with either sulfate groups, sulfoalkyl ether or quaternary amines. These CD's offer a unique ability to stabilize host-guest interactions through electrostatic attractions for oppositely charged enantiomers over a wide pH range. The result is that often enantiomers are more strongly bound and thus only require low CD concentrations to achieve desirable selectivity. It should be noted that higher binding constants do not imply higher selectivity.

Quaternary amine CD's have been used successfully for CE enantiomer separations but as observed by Warner et al. [40] they often cause an undesirable reversal in the direction of the electroosmotic flow. It was proposed in that study that the fixed negative charges at the capillary wall bound the positively charged CD resulting in the capillary wall taking on an overall positive charge. It was also noted in that study that the separation efficiency was unexpectedly low possibly due to chromatographic retention of the analytes by adsorbed quaternary CD.

Weak electrolyte CD's include carboxyalkyl-CD's, aminated CD's and many others. The fact that weak electrolyte CD's are variable in their charge state makes practical method development difficult. However, the ability to change their charge state with changing pH does offer distinct advantages in the separation of mixed chiral

samples as noted by Schmitt and Engelhardt [41]. In this study, the separation of 7 enantio-mer pairs, some basic and some neutral, was achieved using carboxyethyl- β -CD (CBCD) at two pH's. At pH 2.7, CBCD is uncharged and shown to be selective for four of four basic components making up the mixed sample while the neutral components were unresolved. At pH 5.5, CBCD is charged and shown to bind and resolve the three neutral components of the mixed sample while only two of the four basic components were resolved.

The experimental results mentioned thus far all use randomly modified CD's to achieve enantiomer separation. These materials are often poorly characterized and described by their average degree of substitution (d.s.). Randomly modified CD's are complex mixtures of positional isomers with different degrees of substitution. Batch to batch variation of production lots is common resulting in commercially available materials having the same d.s. being composed of different proportions of a large number of positional isomers. Two studies, one by Szemán et al. [42] using CMBCD and another by Francotte et al. using sulfobutylether- γ -CD [43], found that the degree of substitution of the CD dramatically affects chiral resolution in CE. Chankvetadze et al. used ^{13}C NMR to show that different d.s. CD's bind mianserine and its analogues with different enantiospecificity and that indeed the order of migration is dependent on the chiral resolving agent used in the BGE. Each of these authors concluded that working with well characterized CD's is crucial to reliable methods development.

A migration model for enantiomer separations using neutral CD's was first proposed by Rawjee et al. in a series of three papers [44-46] and later extended by

Williams and Vigh to include use of charged resolving agents (CHARM model) [47]. In this model, it was proposed that all enantiomer separations fall into one of three categories; ionoselective separations where only the dissociated forms of the enantiomers complex selectively, desionoselective separations where only the nondissociated forms of the enantiomers complex selectively and duoselective separations where both the dissociated and the nondissociated forms of the enantiomers complex selectively. The model yielded a greater level of understanding of the separations and led to the development of a rational and effective means to separation method development. Results showed that for selectivity optimization of any enantiomer pair with a given chiral resolving agent, one need to know into what category the separations fall. This is accomplished simply by measuring the separation selectivities at both a low and a high pH where the enantiomers are predominately in the protonated and the deprotonated state, respectively. Once the proper pH is known, the chiral resolving agent's concentration is adjusted to maximize separation selectivity followed by adjustment of the EOF mobility to bring about resolution. This methodology was applied to the analysis of the minor enantiomer in L-carbidopa with good results [48]. Maynard and Vigh showed that ionic strength corrections made to the charged resolving agent model (CHARM) explained an unexpected increase in the cationic effective mobility of weakly basic enantiomers in the presence of increasing HMdiSU concentration. Their observations showed that failure to consider the effects of ionic strength potentially leads to poorly developed, less than rugged separations methods [49].

1.3 Single-Isomer Sulfated Cyclodextrins (SiSCD's)

As mentioned before, sulfated cyclodextrins are permanently charged over the entire pH range used in CE and their use in CE does not seem to contribute greatly to chromatographic band broadening effects as do permanently charged quaternary amine CD's. Consequently, SiSCD's are gaining increasing popularity as reliable, effective means to robust enantiomer separations. Several SiSCDs have been used to screen large sets of structurally similar chiral acids, bases, neutrals and ampholytic species under variable CD concentrations and pH conditions in aqueous [50-51] and methanolic [52-55] background electrolytes as well as hydroorganic media [56]. Heptakis(2,3-di-O-acetyl-6-O-sulfo)cyclomaltoheptaose (HDAS) [57] and the corresponding dimethyl (HDMS) [58] and dihydroxy (HDHS)[59] homologs were the first SiSCDs to be used for chiral CE separations. Further research led to the development of two sulfated γ -cyclodextrin species, octakis(2,3-di-O-acetyl-6-O-sulfo)cyclomaltooctaose (ODAS) [60] and the dihydroxy homolog (ODHS) [61], as well as a unique 14 charged CD, heptakis(2-O-methyl-3,6-di-O-sulfo)cyclomaltoheptaose(HMdiSU) [49].

This thesis will present and discuss the synthesis and characterization of a novel SiSCD, the sodium salt of octakis(2,3-di-O-methyl-6-O-sulfo)cyclomaltooctaose (ODMS) for use in both aqueous and nonaqueous CE. It is proposed that this new SiSCD will offer unique selectivity for demanding CE enantiomer separations and contribute to the growing library of available charged chiral resolving agents.

CHAPTER II

SYNTHESIS AND CHARACTERIZATION OF SINGLE-ISOMER ODMS

2.1 Synthesis of SiSCD's

There are several approaches to the synthesis of a single-isomer cyclodextrin. Among the simplest approaches are monomodification, permmodification and a combination of these in a two-step process. These methods have been used to produce various single-isomer neutral as well as charged CD's [62-63]. The reactivity of the 2,3 and 6 hydroxyl groups is such that the 6 position is most reactive in the presence of weak bases like pyridine or dimethylaminopyridine while the 2 position is the one most readily deprotonated in the presence of strong bases such as sodium hydride. The 3 hydroxyl group is least reactive in the presence of both weak and strong bases [64]. The order of reactivity implies that it is also possible to selectively modify the hydroxyl groups in the 2 and 6 position with one functionality followed by selective modification of the hydroxyl group at the 3 position. This strategy has been employed to produce single-isomer, unsymmetrically substituted neutral CD's [65-67].

Another possibility is to selectively protect the hydroxyl group at the 6 position with a suitable protecting group followed by permmodification of all secondary hydroxyl groups. This tactic has been used to produce highly charged CD's which are most desirable for CE separations as predicted by the resolution equation. However, the use of protection group chemistry requires two additional steps in any synthetic method. The potential for undesirable substitution patterns increases with each additional step due to a compounding effect with each successive chemical modification. Figure 3 illustrates the

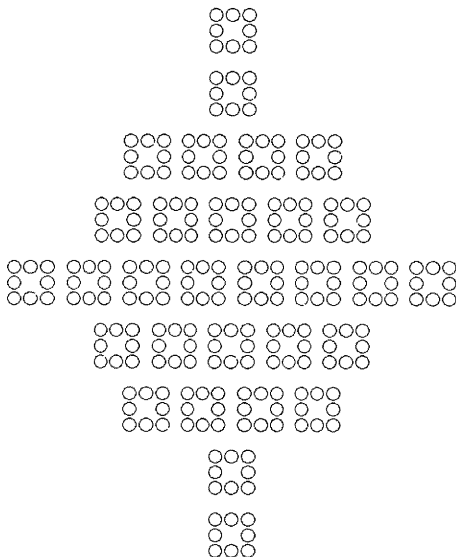


Figure 3. Illustration of the potential substitution patterns observable in the functionalization of the primary hydroxyl groups of native γ -cyclodextrin. Solid circles represent functionalization of any of eight available primary hydroxyl groups.

number of substitution patterns possible in the chemical modification of the primary hydroxyl groups of native γ -CD. Production of a single-isomer requires the purity of the first intermediate to be as high as possible, as further steps will undoubtedly produce multiple substitution patterns of each small impurity formed during the initial protection step.

Synthesis of SiSCD's requires that the hydroxyl groups intended for sulfation be selectively protected while the remaining hydroxyl groups are functionalized as desired. Efficient protection of the primary hydroxyl groups of native CD's with tert-butyldimethylchlorosilane (TBDMS) has been reported. Next, the secondary hydroxyl groups are modified, followed by a deprotection step and then sulfation. This suggests that there are a minimum of four synthetic reaction steps required to produce an SiSCD that is sulfated at the primary hydroxyl groups and modified by some other functionalization at the secondary hydroxyl groups. At each step, there is the potential for the formation of undesirable positional isomers. For this reason, reaction conditions must be carefully controlled as to the relative amounts of the various reagents, and reaction progress must be carefully monitored in an effort to produce only a single isomer.

2.2 Materials and Methods

Native γ -CD was purchased from Wacker Biochem. Corp. (Adrian, MI). Tert-butyltrimethylchlorosilane (97%) was purchased from FMC Lithium Div. (Bessemer City, NC). Imidazole (Im) was obtained from Chem Impex (Wood Dale, IL). Dimethylaminopyridine (DMAP), sodium hydride (60% dispersion in mineral oil), iodomethane and pyridine sulfur trioxide complex and all BGE components were purchased from Aldrich Chemical Co. (Milwaukee, WI). Hydrofluoric acid, and all reaction solvents were obtained from Mallinckrodt Chemical Co. (St. Louis, MO). Activated, 200-mesh, 4Å- molecular sieves were used to dry the solvents. Silica-60 aluminum backed TLC plates from E.M. Science (Gibbstown, NJ) were used for monitoring reaction progress. A reagent solution composed of 35g α -naphthol and 140 mL conc. sulfuric acid in 500mL of an ethanol:water mixture (5.25:1) was used to visualize the cyclodextrin spots. Visualization was accomplished by dipping the TLC plate in the reagent solution and heating it in a 110°C oven for 10 minutes.

An HPLC system consisting of a Beckman 126 solvent module equipped with 6.0 ml/min biopreparative pump heads, a Rheodyne 7125 injection valve (Rheodyne, Cotati, CA), a Eurosep DDL-31 evaporative light scattering detector (Eurosep Instruments, St. Christophe, France) set to 53°C and 400 gain and a Beckman 406 A/D converter operated under Gold 8.1 chromatography software (Beckman-Coulter, Fullerton, CA) on an IBM PS/2 PC was used to establish the purity of all intermediates. Separations were carried out with various ethyl acetate/methanol mixtures on 4.6mm i.d. x 250mm analytical columns packed with either 5 μ m Luna silica or 5 μ m Luna C18 stationary

phases. Response factors for all eluting peaks were assumed to be equal.

Analysis of the isomeric distribution of the final product was done using either a Beckman P/ACE 2100 or P/ACE 5000 system equipped with a UV detector operated at 214 nm on a 26cm long, 25 μ m i.d. bare fused silica capillary (injector to detector length 19 cm) (Polymicro Technologies, Phoenix, AZ), at 20kV separation potential and (-) to (+) polarity. The BGE used was 30mM tetramethylethylenediamine titrated to pH 8.1 with para-toluenesulfonic acid. The reaction was sampled while in progress, diluted with the BGE and the solution was injected for 1 sec at 1 p.s.i. before application of the separation potential. All analyses were completed at 20°C.

1-D NMR experiments were done on a Varian 300MHz UnityPlus Spectrometer (Varian Assoc., Walnut Creek, CA) equipped with a $^1\text{H}/^{19}\text{F}/^{31}\text{P}/^{13}\text{C}$ quad probe using Solaris 2.4 software running on a SUN workstation. 2-D experiments including double quantum filtered ^1H - ^1H correlation spectroscopy (DQ-COSY) and ^1H - ^{13}C heteronuclear correlation spectroscopy (HETCOR) were obtained on either the same 300MHz UnityPlus Spectrometer or on a Varian 500 MHz UnityPlus spectrometer equipped with $^1\text{H}/^{13}\text{C}$ dual tunable probe and VnmrX 5.3b software running on a SUN workstation.

High-resolution MALDI-TOF mass spectra were obtained with a Voyager Elite XL mass spectrometer equipped with delayed extraction capability (Perceptive Biosystems, Framingham, MA) with the following instrument settings: nitrogen laser ($\lambda = 337$ nm), reflectron mode, 25 kV acceleration voltage, 70% grid voltage, 0.030% guide wire voltage and 180 μ s delay time. The mass spectra from 60 to 80 laser pulses were averaged to achieve adequate signal-to-noise ratio. All samples were prepared by

dissolving 10 mg of 2,4,6-trihydroxyacetophenone (THAP) in 1 mL HPLC grade acetonitrile and 10 mg of the cyclodextrin derivative to be analyzed in 1 mL of either CH_2Cl_2 or water, along with 10 mg of an internal standard, heptakis(2-O-methyl) cyclomaltoheptaose. Equal volumes of these solutions were combined and 10 μL applied to a PTFE target stage and allowed to dry [68].

Crystal structures were obtained on a Bruker SMART 1000 X-ray diffractometer (Bruker AXS, Madison, WI) from single crystals grown in suitable solvents. Diffraction patterns were solved and refined using the SHELXL program suite running on a Pentium III 300 MHz processor PC. Crystal structure and Connolly surface figures were generated using the Insight II molecular modeling software package running on an SGI O_2 workstation.

2.3 Synthesis and Characterization of ODMS and Its Intermediates

The four step methodology to produce the single-isomer sulfated cyclodextrin, the sodium salt of octakis(2,3-di-O-methyl-6-O-sulfo)cyclomaltooctaose on large scale is shown in Figure 4. The use of protection group chemistry allowed for regioselective sulfation and permethylation of the primary and secondary hydroxyl groups, respectively. The details of the synthetic procedure are included in appendix B.

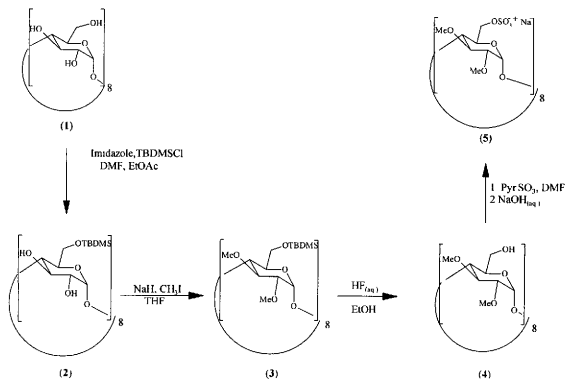


Figure 4. Synthetic scheme for octakis(2,3-di-O-methyl-6-O-sulfo)cyclomaltooctaose.

2.3.1 Octakis(6-O-*t*-butyldimethylsilyl)cyclomaltooctaose

Protection of the primary hydroxyl group at the 6 position of (**1**) in DMF at room temperature was achieved with TBDMS in ethyl acetate (EtOAc) according to a modified procedure of Takeo [69]. The reaction was monitored by TLC with a 50:15:1 CHCl₃:MeOH:H₂O mobile phase giving an $R_f = 0.57$ for the target compound. Accurate analysis of the purity of the product was achieved using a 5 μ m Luna C18 RP-HPLC column with a 35:65 MeOH:EtOAc isocratic mobile phase at 2 mL/min. A total of 4 kg of native γ -cyclodextrin was silylated in this manner and recrystallized from both methanol and acetone to yield a 99.2% isomerically pure white powder. The total crystalline yield was 4.572 kg corresponding to a 67% yield of the theoretical value. A ¹H NMR spectra of (**2**), included as Figure 5, is in good agreement with published values. The high resolution MALDI-TOF mass spectrum of the sodium adduct of (**2**) is shown in Figure 6. The measured mass to charge (m/z) value of 2231.72 agrees well with the value calculated for the monoisotopic [C₉₆H₁₉₂O₄₀Si₈Na]⁺, 2232.10. Single crystals were grown from acetone and used for X-ray diffraction analysis. The crystal structure of (**2**) is included as Figure 7.

2.3.2 Octakis(2,3-di-O-methyl-6-O-*t*-butyldimethylsilyl)cyclomaltooctaose

The secondary hydroxyl groups of (**2**) were methylated in THF at room temperature using iodomethane and NaH (60% dispersion in oil) for 4 h to obtain (**3**) with 97% conversion at the 250 g scale. Reaction progress was monitored using a 5 μ m Luna C18 RP-HPLC column with a 50:50 MeOH:EtOAc isocratic mobile phase at 2 mL/min. No suitable, large scale recrystallization solvent was found. Assigned ¹H and

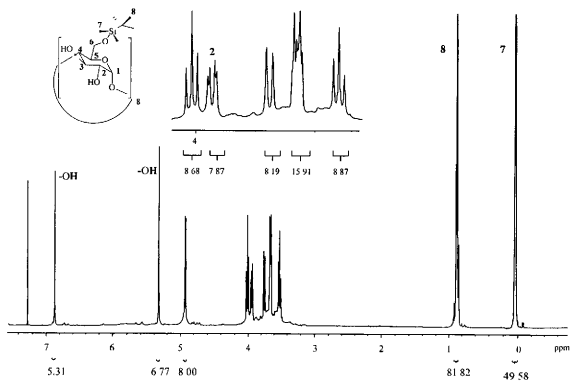


Figure 5. $^1\text{H-NMR}$ spectrum of (2) in CDCl_3 .

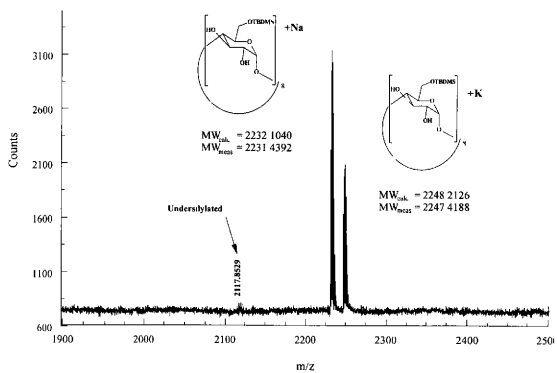


Figure 6. A section of the MALDI-TOF mass spectrum of (2).

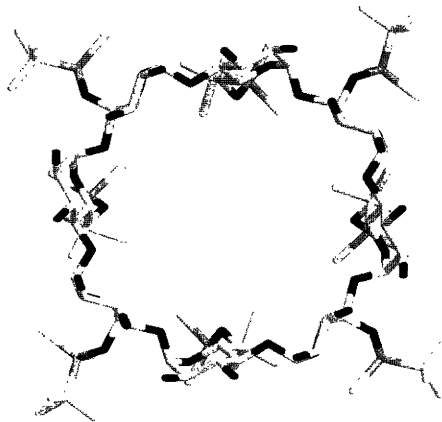


Figure 7. Crystal structure of (2).

^{13}C NMR spectra of (3) are included as Figure 8. The high resolution MALDI-TOF mass spectrum of the sodium adduct of (3) is shown in Figure 9. The measured m/z value of 2455.73 agrees well with value calculated for the monoisotopic $[\text{C}_{112}\text{H}_{224}\text{O}_{40}\text{Si}_8\text{Na}]^+$, 2456.35. Single crystals were grown from DMF and used for X-ray diffraction analysis. The crystal structure of (3) is included as Figure 10 along with Connelly solvent surface.

2.3.3 Octakis(2,3-di-O-methyl)cyclomaltooctaose

Deprotection of (3) was accomplished using 48% HF_{aq} in anhydrous ethanol for 12 h at room temperature to obtain (4) with 96 % conversion at the 400 g scale. The reaction was monitored by TLC with a 50:15:1 CHCl_3 :MeOH:H₂O mobile phase giving an $R_f = 0.52$ for the target compound. Accurate analysis of the purity of the product was done using a 5 μm Luna Silica NP-HPLC column with a 80:20 EtOAc:MeOH isocratic mobile phase at 2 mL/min. The crude material was recrystallized 6 times from acetone to yield a 99.2% isomerically pure white powder. Several reactions were done on the 400 g scale for an average yield of 72% of the theoretical. Assigned ^1H and ^{13}C NMR spectra of (4) are included as Figure 11. The high resolution MALDI-TOF mass spectrum of the sodium adduct of (4) is shown in Figure 12. The measured m/z value of 1543.91 agrees well with the value calculated for the monoisotopic $[\text{C}_{64}\text{H}_{112}\text{O}_{40}\text{Na}]^+$, 1544.66. Single crystals were grown from acetone and used for X-ray diffraction analysis. The crystal structure of (4) is included as Figure 13.

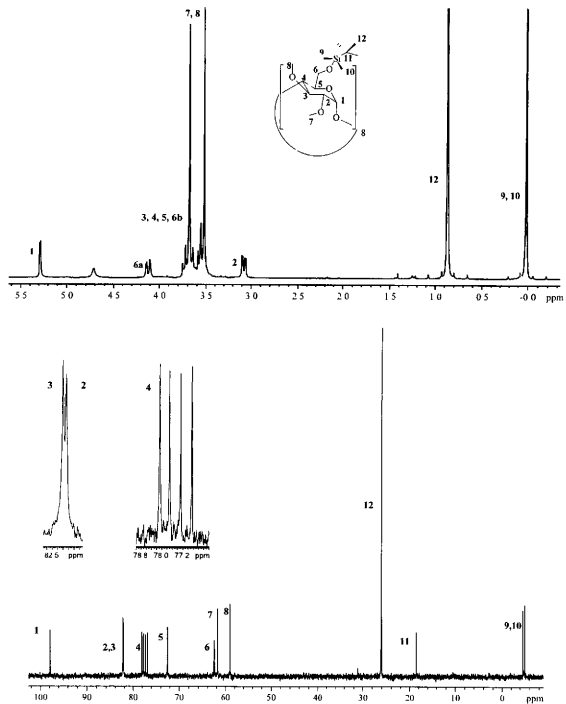


Figure 8. Assigned ¹H and ¹³C-NMR of (3) in CDCl₃.

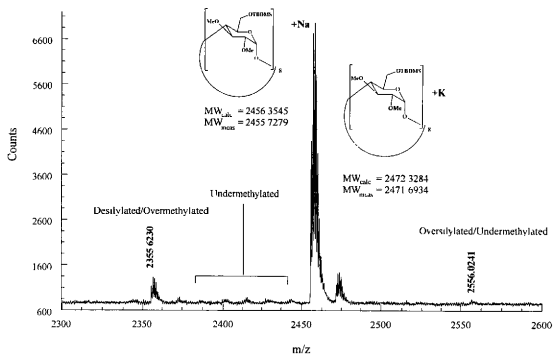


Figure 9. A section of MALDI-TOF mass spectrum of (3).

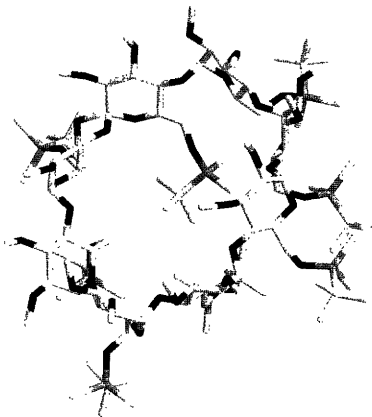


Figure 10. Crystal structure of (3).

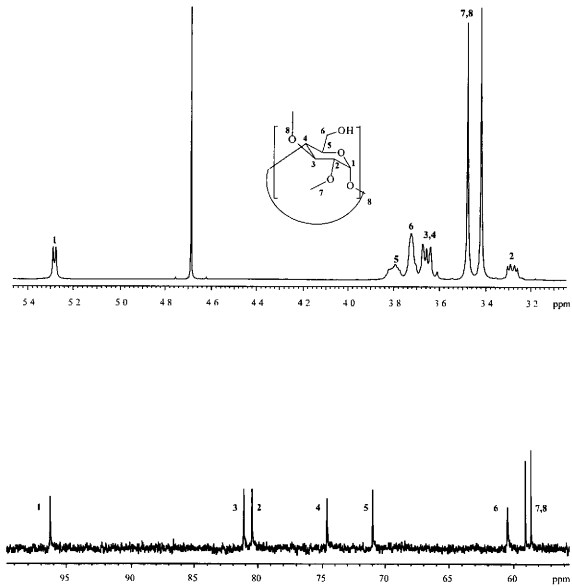


Figure 11. Assigned ¹H and ¹³C-NMR of (4) in D₂O.

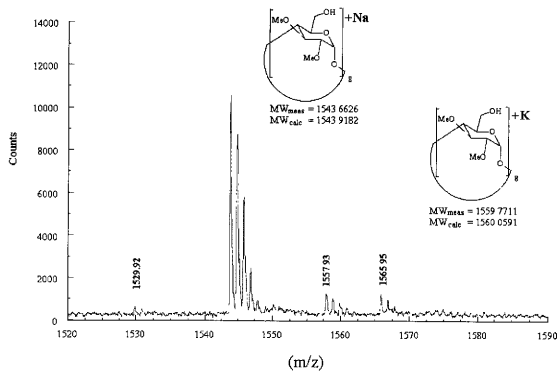


Figure 12. A section of the MALDI-TOF mass spectrum of (4).

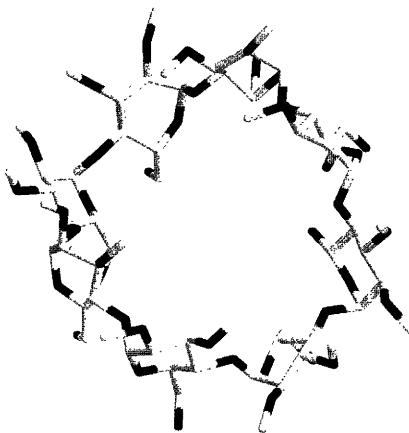


Figure 13. Crystal structure of (4).

2.3.4 Octakis(2,3-di-O-methyl-6-O-sulfo)cyclomaltooctaose

Sulfation at the 6 position of (**4**) was done in DMF at room temperature for 0.5 h using pyridine sulfur trioxide complex to obtain (**5**) with 93% conversion at the 250 g scale. The reaction was monitored by indirect UV detection CE analysis in 30 mM tetramethylethylenediamine BGE titrated to pH 8.1 with para-toluene sulfonic acid with (+) to (-) polarity. Purification of the crude material was accomplished by 6 precipitations from a 6:1 ethanol:water mixture by dissolving the crude material in a minimum volume of water followed by addition of six times the water volume of 200 proof ethanol. The final isomeric purity of the white powder obtained was found to be >98% by indirect UV detection CE as indicated in Figure 14. Assigned ^1H and ^{13}C NMR spectra of (**5**) included as Figure 15 show that the product is free of reaction solvent. The high resolution MALDI-TOF mass spectrum of the sodium adduct of (**5**) is shown in Figure 16. The measured m/z value of 2359.16 agrees well with the value calculated for the monoisotopic, $[\text{C}_{64}\text{H}_{104}\text{O}_{64}\text{S}_8\text{Na}_9]^+$, 2359.17. Single crystals were grown from ethanol water and used for X-ray diffraction analysis. The crystal structure of (**5**) is included as Figure 17 along with the Connelly solvent surface. Analysis for $\text{C}_{64}\text{H}_{104}\text{O}_{64}\text{S}_8\text{Na}_8 \cdot 16\text{H}_2\text{O}$ calcd: C, 29.27; H, 5.22; O, 48.74; S, 9.77. Found: C, 29.37; H, 5.26; O, 48.68; S, 9.66.

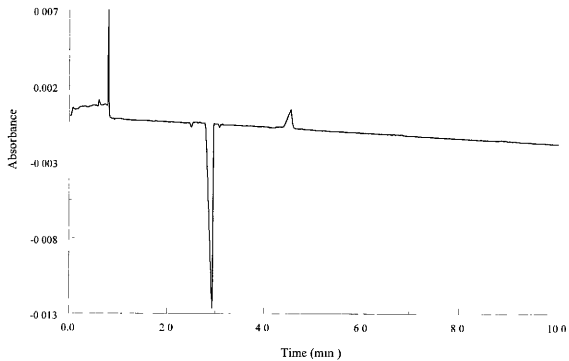


Figure 14. Indirect UV-detection CE of recrystallized (**5**). Positive-going peaks are EOF peak (at < 1 min) and a system peak (at 4.5 min). Final isomeric purity is > 98%.

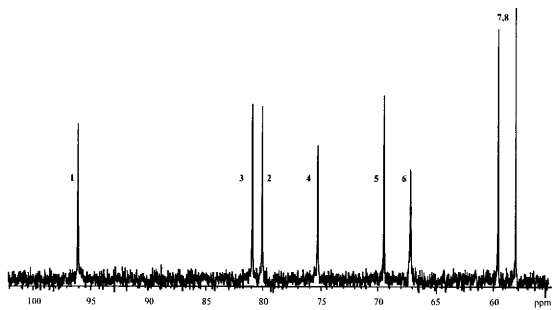
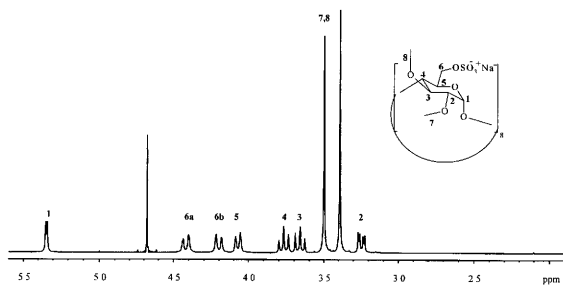


Figure 15. Assigned ^1H and ^{13}C -NMR of (5) in D_2O .

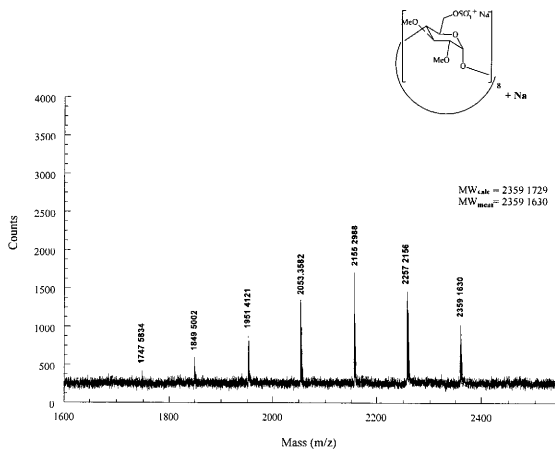


Figure 16. A section of the MALDI-TOF mass spectrum of (5).

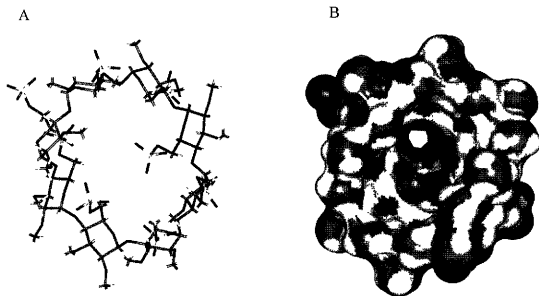


Figure 17. Crystal structure (A) and Connolly solvent surface (B) of (5).

2.4 Discussion of Synthetic Results

The reaction sequence used to produce single isomer ODMS began with the selective protection of the primary hydroxyl groups of native γ -cyclodextrin. TBDMS was chosen as the protecting group because it is a sufficiently stable, silicon based protecting group. The remaining synthetic steps were chosen for the production of single- isomer ODMS for their ease of scalability and simple, fast, efficient work-up conditions. Recrystallization of intermediates proved to be adequate for purification and the more costly, both in time and materials, chromatographic techniques could be avoided. Choice of recrystallization solvents was limited to low cost, low toxicity solvents. These requirements eliminated DMF as a possible recrystallization solvent even though this was the only solvent suited to the recrystallization of (3). The side products observed in the synthesis of (3) could be removed in subsequent synthetic steps.

Recrystallization of (2) was done from both acetone and methanol. Acetone recrystallizations afforded (2) while the over-silylated side product was retained in the mother liquor. Methanol recrystallizations afforded (2) while the under-silylated side product was retained in the mother liquor. Nonaqueous RP-HPLC was used to monitor the purity of (2) throughout recrystallization. Figure 18 is a comparison of chromatographic traces obtained for the reaction product prior to recrystallization and after recrystallization. A sample made by mixing both the acetone and methanol mother liquors afforded a sample that was enriched in all observed impurities. This sample was used to construct a Horvath plot shown in Figure 19. Here, the logarithm of the retention factor (k') of each component of the mixed sample is plotted as function of eluent

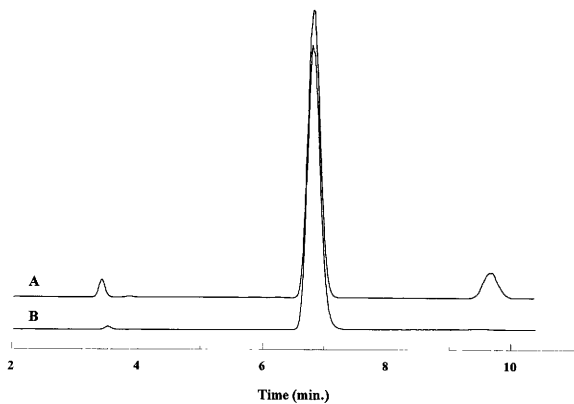


Figure 18. ELSD traces of (1) (A) prior to recrystallization and (B) after recrystallization.

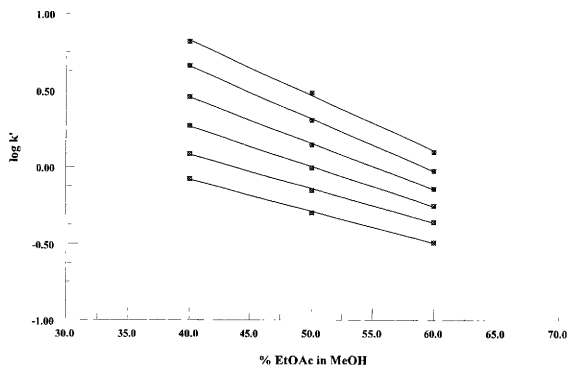


Figure 19. Horvath plot of components of a sample obtained by mixing acetone/methanol mixed mother liquors.

composition (%EtOAc). Retention factor (k') of each component of the mixed sample is plotted as function of eluent composition (%EtOAc). The $\log k'$ vs. %EtOAc plots are linear for each component indicating reversed phase chromatographic behavior.

One dimensional ^1H NMR was used to show that any impurity with mono-substitution at the secondary hydroxyl groups was not present in the final recrystallized material. Figure 20 shows the ^1H NMR in the -0.2 to 1.2 ppm range of a sample containing both the desired eight fold substituted product and the nine fold substituted side product in equal proportions. The peaks at δ 0.09 and δ 0.91 in the ^1H NMR spectrum correspond to $\text{C}(\text{CH}_3)_3$ and $\text{Si}(\text{CH}_3)_2$, respectively, of the impurity with a single substitution of the secondary hydroxyl groups. Integration values are 8:1 for target: impurity peaks. The same peak pattern was observed in the ^1H -NMR of a protected β -CD, also included in Figure 20, where all of the primary hydroxyl groups were protected and one-half of the secondary hydroxyl groups were protected at the 2 position. This evidence shows conclusively that co-elution of undesirable side products is of little concern and that HPLC analysis of the recrystallized product provided an accurate measure of purity.

Methylation of (**2**) yielded predominantly one isomer at 98% conversion after optimization of the reaction conditions. The MALDI-TOF mass spectrum (see figure 9) indicated the presence of a species with a measured m/z value of 2355.62. This agrees well with the value calculated for the monoisotopic $[\text{C}_{107}\text{H}_{212}\text{O}_{40}\text{Si}_7\text{Na}]^+$, 2356.28 for the monodesilylated and subsequently over-methylated product. It was found that the relative

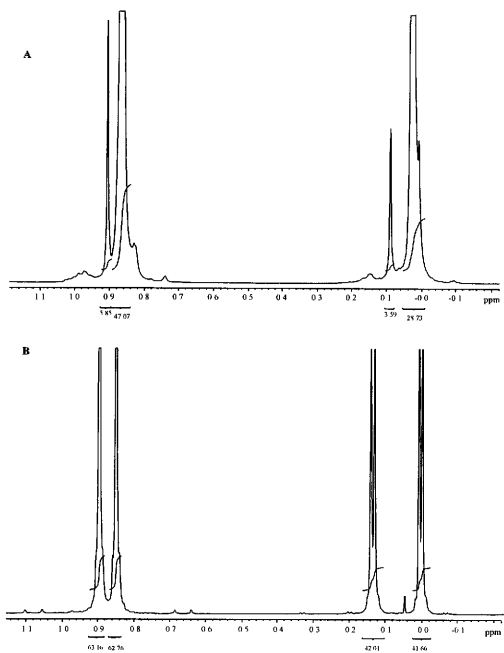


Figure 20. Comparison of $^1\text{H-NMR}$ spectra of (2) (A) with known over-silylation impurity and (B) of a previously well characterized 14-silylated β -CD.

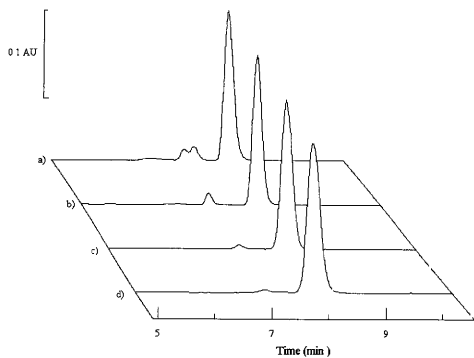


Figure 21. ELSD traces for the optimization of the methylation of (2). Conditions are: a) 1.2 mol excess CH_3I , 1.8 mol excess NaH , b) 1.5 mol excess CH_3I , 1.8 mol excess NaH , c) 1.5 mol excess CH_3I , 1.5 mol excess NaH and d) 1.5 mol excess CH_3I , 1.2 mol excess NaH .

amount of the side-product formed in the reaction was reduced from 8% to 2% by adjusting the amount of sodium hydride from 1.8 molar excess to 1.2 molar excess as shown in Figure 21, and limiting the reaction time to only 5 h.

Impurities due to incomplete deprotection of (3) as well as those impurities formed during the previous synthetic step were removed in 6 recrystallizations from acetone. The MALDI-TOF mass spectrum of (4) (see figure 13) indicates the presence of at least a small amount of under-methylated product, as well as another impurity whose measured m/z value of 1565.95 corresponds to $[C_{64}H_{111}O_{40}Na_2]^+$; a monodeprotonated/monosodiated sodium adduct with an overall positive one charge. This species could be an artifact of the MALDI process however, it could also be produced in the basic work-up of the reaction mixture. Conclusive identification of this peak is not possible as there is no discernible peak for the corresponding monodeprotonated/ monosodiated potassium adduct.

Attempts to monitor the sulfation of (4) were difficult as this proved to be a very fast reaction. Partially reacted samples made by the addition of substoichiometric amounts of the sulfating reagent to (4) in DMF were used for development of a suitable CE separation method. The electropherograms in Figure 22 show that the chosen method of analysis is well suited to monitoring the sulfation reaction. In each case, a stable, low noise baseline is obtained. Peaks for the more highly substituted species are sharp and well resolved. The more slowly migrating components are partially resolved positional isomers that are equal in charge but differ in the size of their respective hydration spheres. It is a valuable observation that, at least in the BGE used for this analysis,

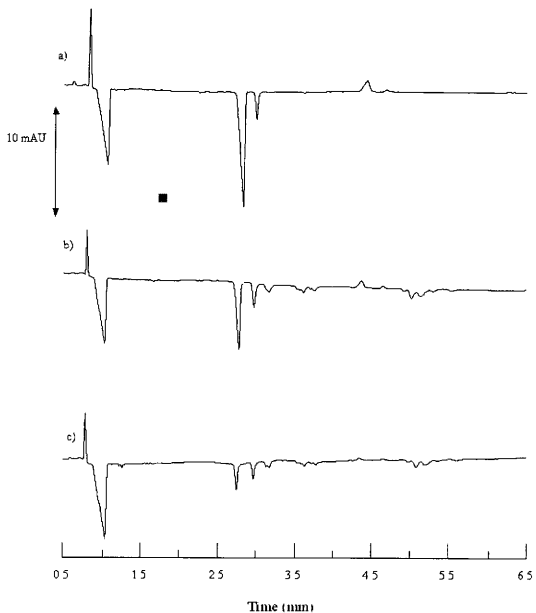


Figure 22. Evaluation of the suitability of indirect UV-detection CE for use in monitoring the sulfation of (4). Conditions are: a) 100%, b) 75% and c) 50 % addition of the stoichiometric amount of pyridine sulfur trioxide complex to (4) in DMF.

Mixture of randomly substituted CD's used for enantiomer separations are composed of species that potentially differ not only in their molecular structure, and therefore their enantio-recognition properties, but also in their electrophoretic behavior.

^1H and ^{13}C NMR assignments of all reaction intermediates were made from DQ-COSY and HETCOR two-dimensional NMR experiments. A DQ-COSY pulse sequence was required to establish ^1H - ^1H connectivities as opposed to a simple COSY pulse sequence due to occasional overlap of coupled signals with non-coupled signals. Figure 23 is an example of the DQ-COSY spectra obtained for (5) where ^1H - ^1H connectivities are indicated by alignment of diagonal peaks with off-diagonal crosspeaks. The DQ-COSY pulse sequence effectively suppressed the non-coupled methyl ether signals observed along the diagonal in the one-dimensional experiments. An example of an HETCOR experiment is included as Figure 24 where ^1H - ^{13}C connectivities are indicated by vertical and horizontal alignment of crosspeaks with peaks observed in the one dimensional spectra shown at each axis.

MALDI-TOF mass spectral analysis of (5) showed that while the MALDI process is a "soft" ionization technique capable of producing more non-fragmented molecular ions with only a single charge than electron impact techniques, fragmentation was still observed for single isomer ODMS (see figure 16). A total of seven peaks were observed with a constant peak difference of 101.90 corresponding to successive loss of SO_3Na and gain of a single proton. This result shows that MALDI-TOF mass spectrometry is limited to measurement of the mass of the most highly sulfated species present and cannot be used to evaluate the degree of substitution of the product. No over-sulfated species

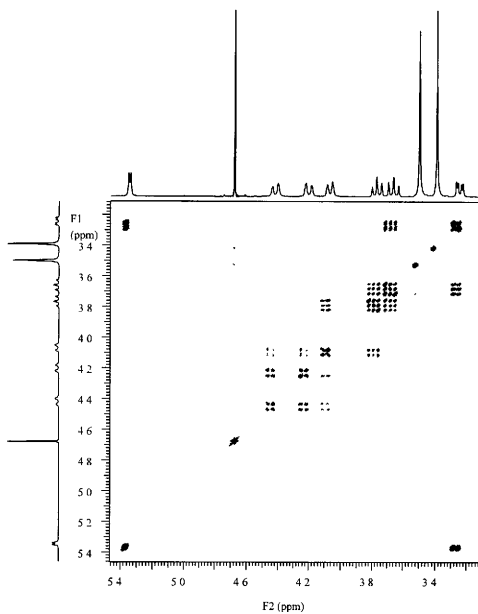


Figure 23. DQ-COSY spectrum of (5) in D₂O.

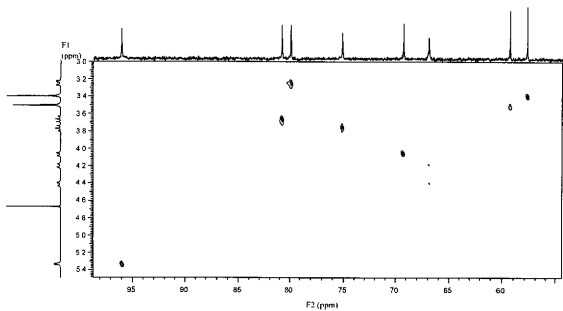


Figure 24: HETCOR spectrum of (5) in D₂O.

were observed in this measurement.

The final step to producing well characterized, single-isomer ODMS is the removal of a contaminant, Na_2SO_4 , through its selective precipitation and subsequent filtration from a concentrated solution in methanol. The filtrate is evaporated to dryness to yield a material containing less than 0.1% Na_2SO_4 . This is a vital step in the purification of ODMS as any ionizable contaminant will contribute to the ionic strength of solutions of ODMS used for CE enantiomer separations.

2.5 Summary

The large-scale preparation of the sodium salt of octakis(2,3-di-O-methyl-6-O-sulfo)cyclomaltooctase for use as a single-isomer chiral resolving agent in capillary electrophoretic separation of enantiomers has been accomplished through a four step synthetic methodology. The steps used consist of well known chemical transformations beginning with a critical protection step which allowed for reliable and predictable modification of the large number of available substitution sites. The final product, along with each intermediate has been extensively characterized by analytical methods including HPLC-ELSD, indirect UV detection CE, MALDI-TOF MS, 1D and 2D NMR and X-ray diffraction crystallography to show that, indeed, a single-isomer SiSCD was produced.

CHAPTER III

ENANTIOMER SEPARATIONS

3.1 Use of ODMS as a Chiral Resolving Agent

ODMS was used as a chiral resolving agent for the CE separation of the enantiomers of 78 racemic and nonracemic weakly acidic, weakly basic and nonionic compounds, most of which are pharmaceutically active. Separation selectivity was determined in various BGE's as a function of the concentration of the chiral resolving agent. The effective mobilities (μ^{eff}) and normalized electroosmotic mobilities (β) were calculated per equations 3 and 5 (see Chapter I), respectively. Effective mobilities and separation selectivities were plotted as a function of the ODMS concentration to evaluate both the best pH and concentration for the highest available separation selectivity (α), also defined in Chapter I. Peak resolution was calculated from peak half-height widths (w^h) as $Rs = [2(t_2 - t_1)] / [1.699(w_2^h + w_1^h)]$. Whenever possible, qualitative comparisons were made between the separations achieved in aqueous and non-aqueous BGE's.

3.2 Materials and Methods

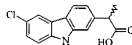
All chiral analytes listed in Figures 25-27 were obtained from either Sigma (St. Louis, MO), Aldrich Chemical Co. (Milwaukee, WI), Wiley Organics (Coshocton, OH) or Research Diagnostics (Rockdale, MD). Dimethylsulfoxide (DMSO) and HPLC grade methanol were purchased from EM Science (Gibbstown, NJ). Aqueous solutions were

Part of the material in this chapter is reprinted with permission from:

M. Brent Busby, Omar Maldonado, and Gyula Vigh, *Electrophoresis*, 23 (2002) 456-461; Copyright 2002-Wiley-VCH.



A02: trans-2-Phenyl-1-cyclopropane carboxylic acid

A03: α -Methyl- α -phenylsuccinimide

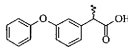
A04: Carprofen



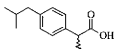
A16: Ethosuximide



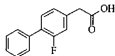
A16: 5-(4-methylphenyl)-5-phenylhydantoin



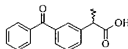
A22: Fenoprofen



A23: Ibuprofen



A26: Flurbiprofen



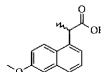
A27: Ketoprofen



A28: Mandelic acid



A30: 2-phenyl-3-methylvaleric acid



A31: Naproxen



A36: 2-Phenylpropionic acid

Figure 25. Names and structures of weak acid analytes.

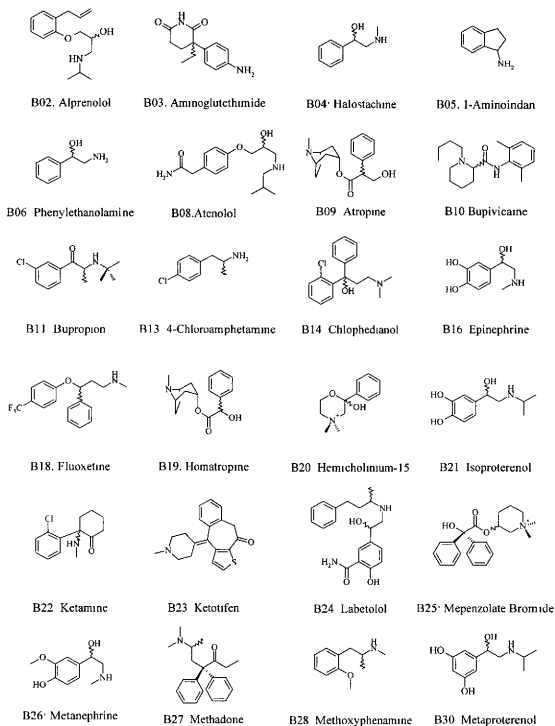
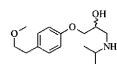


Figure 26. Names and structures of weak base analytes.



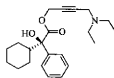
B31 Metoprolol



B33 (1-Naphthyl)ethylamine



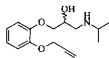
B34 Norephedrine



B35 Oxycbutynn



B36 Oxypheyclimine



B37 Oxprenolol



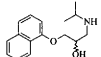
B38 Piperoxan



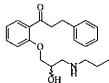
B39 Phenylglycinonitrile



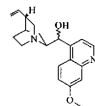
B41 Pindolol



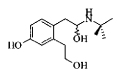
B42 Propranolol



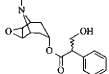
B43 Propafenone



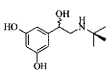
B44 Quinidine



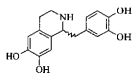
B45 Salbutamol



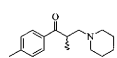
B46 Scopolamine



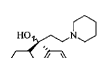
B47 Terbutaline



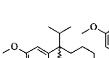
B49 Tetrahydropapaveroline



B51 Tolperisone



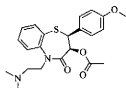
B53 Trihexylphenidyl



B54 Verapamil



B56 Chlorpheniramine



B57 Diltiazem



B58 Tetrahydrozoline



B60 Ephedrine

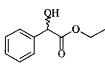


B61 Synephrine

Figure 26. Continued



N02: 2-Phenylbutanol



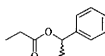
N10: Ethylmandelate



N15: Methylmandelate



N19: Pantolactone



N20: 1-Phenylethylpropionate



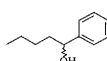
N21: 1-Phenylbutanol



N22: 3-Phenylbutyraldehyde



N24: Styrene glycol



N25: 1-Phenylpentanol



N26: 2-Phenyl-2-pentanol



N30: trans-2-Phenyl-1-cyclohexanol



N34: 1-Phenylpropanol



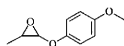
N36: 1-Indanol



N38: 2-Phenyl-2-butanol



N39: 2-Phenylpropionaldehyde



N40: 2,3-Epoxypropyl-4-methoxyphenylether

Figure 27. Names and structures of non-ionic analytes.

prepared from deionized water obtained from an in-house Milli-Q unit (Millipore, Milford, MA). All solutions were filtered prior to use with a 0.45 μm Gelman nylon membrane filter (VWR, South Plainfield, NJ). Nitromethane (NM), phosphoric acid, lithium hydroxide, ethanolamine and methanesulfonic acid were purchased from Aldrich Chemical Co. ODMS was prepared as described in Chapter II.

Capillary electrophoretic measurements were made using either a P/ACE 2100 or P/ACE 5000 CE instrument with its UV detector set to 214 nm. A 46 cm total length (39 cm to detector), 25 μm i.d., naked fused-silica capillary was used for the aqueous measurements, a 26 cm total length (19 cm to detector), 25 μm i.d., naked fused-silica capillary for the nonaqueous measurements. Aqueous BGE's included one buffered at low pH with 20 mM H_3PO_4 ($\text{pK}_{\text{a}1}$ 2.1), titrated to pH 2.5 with LiOH, and another buffered at high pH with 20 mM ethanolamine (pK_{a} 9.5), titrated to pH 9.5 with methanesulfonic acid. An acidic methanolic buffer was prepared from 20 mM H_3PO_4 and 10 mM NaOH for use in nonaqueous measurements. The stock buffers were used to prepare the 0-40 mM ODMS BGE's for CE enantiomer separations. The enantiomers were dissolved in the BGE and co-injected for 1 s by 1 psi nitrogen with the EOF marker from a solution approximately 0.5 mM in both the analyte and the marker. All measurements were repeated in triplicate. Ohm's plots were measured from 0-50 mM ODMS at 5 mM ODMS increments in each BGE. Effective mobility measurements were carried out within the linear region of Ohm's law. The effective mobilities of the enantiomers were measured against the neutral markers, nitromethane (NM) at low pH and DMSO at high pH, neither of which possess an intrinsic charge and thus, have zero

effective mobility at the pH of their respective BGE's. Also, neither of these neutral markers indicated complexation-induced mobility in their respective BGE's according to the modified external mobility marker method colloquially referred to as the sandwich method [70], detailed in figure 28 and in the following text. Figure 29 is an example of a measurement obtained at the highest ODMS concentration used in the low pH BGE for NM. The analyte whose complexation-induced mobility is to be measured is dissolved in both ODMS-containing BGE and in ODMS-free BGE. The capillary used for this measurement is equal in length on both sides of the detector window so that the analyte bands placed before the detector can be pushed via nitrogen pressure past the detector and still remain within the capillary. The capillary is filled in its entirety with the ODMS-free BGE (step a) followed by a 1-2 min injection of the ODMS-containing BGE (step b). Next, the analyte dissolved in the ODMS containing BGE is injected (step c) followed by another 1-2 min injection of the ODMS-containing BGE (step d). Next, ODMS-free BGE is injected for 1-2 min, followed by the injection of two plugs of the analyte dissolved in the ODMS-free BGE, separated from one another by a 1-2 min injection of the ODMS-free BGE (steps e through h). Thus, a region of the capillary is filled by the ODMS-containing BGE sandwiched between two regions of the ODMS-free BGE. All injection periods are adjusted so that none of the ODMS-containing BGE is pushed past the detector window while the remaining injection sequences are performed. At this point, content of the entire capillary is pressure mobilized past the detector to obtain a UV trace indicating the initial distance between the analyte plugs in the two BGE's. After all analyte plugs move past the detector, the content of the

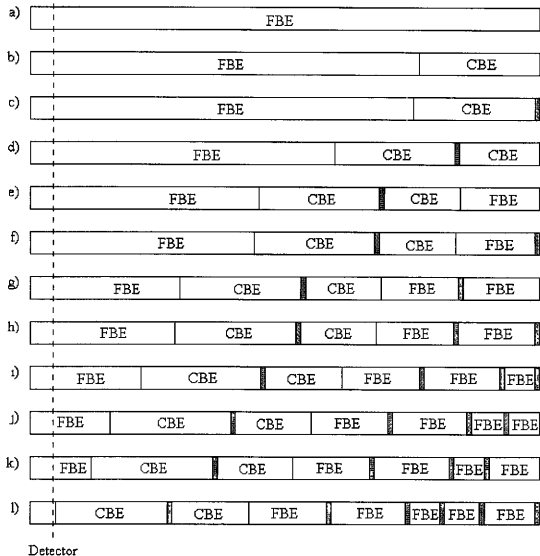


Figure 28. Injection sequence for sandwich method. FBE: ODMS-containing BGE, CBE:

ODMS-free BGE, analyte injections are solid bands.

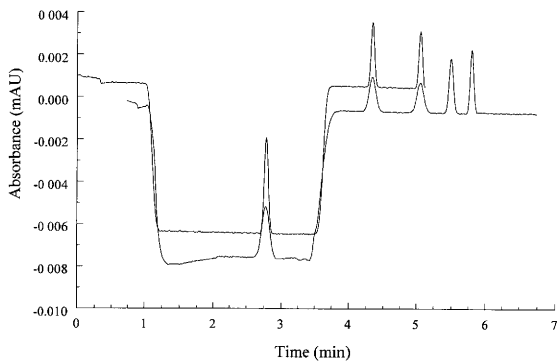


Figure 29. Sandwich method overlays. Example of results from sandwich run with low pH BGE. Analyte peaks are NM.

capillary is returned to the injection side of the capillary by pressure mobilization in the reverse direction, followed by another injection of the analyte in the ODMS-free BGE (step i). Then, the content of the capillary is pressure mobilized toward the detector with ODMS-free BGE to make certain that all analyte plugs are within the thermostated region of the capillary (step j). Next, a potential is applied to the capillary for a period not long enough to allow any portion of the ODMS-containing BGE section to migrate past the detector window (step k). After the electrophoretic period is complete, the content of the capillary is again pressure mobilized past the detector window (step l) to obtain a UV trace indicating the post-electrophoresis distance between the analyte plugs. Finally, the pre- and post-electrophoresis UV traces are overlaid using the two peaks within the ODMS-free BGE as reference and the distance between the analyte plugs in the charged BGE are compared. If the two analyte peaks in the ODMS-containing BGE region do not line up, ODMS complexed with the analyte and caused its migration. If the same two peaks do line up, it is concluded that ODMS did not complex with the analyte measurably.

Figure 29 indicates that nitromethane is suitable for use as an EOF marker for effective mobility measurements in the low pH BGE's when the ODMS concentration is lower than 40 mM. Similar conclusion was obtained for DMSO in the high pH ODMS-containing BGE.

3.3 Aqueous Separations

Effective mobilities for moderate molecular weight ($200 < MW < 500$), singly-charged compounds usually lie in the $\pm 25 \times 10^{-5} \text{ cm}^2\text{V}^{-1}\text{s}^{-1}$ range. Consequently, use of

low pH BGE's, where μ^{eo} values are around $+10 \times 10^{-5} \text{ cm}^2\text{V}^{-1}\text{s}^{-1}$ to $+25 \times 10^{-5} \text{ cm}^2\text{V}^{-1}\text{s}^{-1}$ in naked fused silica capillaries, is conducive to good resolution because more favorable β values are obtained than in high pH BGE's where typical μ^{eo} values are higher than $+50 \times 10 \text{ cm}^2\text{V}^{-1}\text{s}^{-1}$. Previous work has shown that, in the molecular weight range specified, complexation with SiSCD's commonly leads to mobilities as high as -25 mobility units ($\times 10^{-5} \text{ cm}^2\text{V}^{-1}\text{s}^{-1}$) and occasionally as high as -50 mobility units. This means that it is possible to adjust the concentration of SiSCD's to bring about an effective mobility for weakly basic enantiomers that is nearly equal in magnitude but opposite in direction to the electroosmotic flow mobility and thus, take advantage of even the lowest separation selectivity to achieve a desirable resolution. For these reasons, evaluation of the potential of a new SiSCD to be used as a chiral resolving agent almost always begins with the separation of weakly basic enantiomers in low pH BGE's.

3.3.1 Weakly Basic Enantiomer Separations in Aqueous BGE's

A set of 46 pharmaceutically active, weakly basic enantiomers were used to evaluate the utility of ODMS as a chiral resolving agent in low pH aqueous BGE's. A total of 36 enantiomers showed some measure of separation selectivity in either low or high pH aqueous BGE's. Only one of the 36 was separated at high pH and not at low pH. At low pH, the applied potential was limited to 27 kV in the 5mM ODMS-containing BGE and decreased with increasing ODMS concentration to 9kV in the 40 mM ODMS-containing BGE. Likewise, at high pH, the applied potential was limited to 12 kV in the 5 mM ODMS-containing BGE and decreased to 8 kV in the 40 mM ODMS-containing BGE. These potential differences reflect the conductivity differences of the BGE's.

Under these conditions, μ^{co} values were about 12 to 18 mobility units in the low pH BGE's over the entire ODMS concentration range, and decreased from about 40 mobility units in the 5mM ODMS-containing, high pH BGE to about 18 mobility units in the 40 mM ODMS-containing, high pH BGE.

The speed with which the separations were completed (generally under 25 min) was in part due to the aid of the EOF but, the greatest factor was the weak binding between ODMS and the enantiomers, because, at low pH, most of the bases maintained their cationic mobility. Separations in the high pH BGE's were also fast, but for opposite reasons. The EOF mobility is considerably higher at high pH due to the increased charge density of the capillary wall while the enantiomers are much less cationic in nature because of their lower degree of protonation. As the ODMS concentration is increased in the high pH BGE's, the enantiomers typically acquire an anionic effective mobility at considerably lower ODMS concentrations than in the low pH BGE and migrate against the EOF mobility. The result is that, in most cases, the enantiomers migrate with an observed mobility between 15 and 30 mobility units. This leads to separation times between 5 and 25 min, depending on the applied potential.

At low pH, observed mobilities indicate that the weakly basic enantiomers can be classified into two categories: weakly binding and strongly binding. For the purposes of this discussion, a weakly binding base is one whose low pH mobility remains cationic at all tested ODMS concentrations. The mobility and separation selectivity curves of three weakly binding basic enantiomers are shown in Figure 30. In each case, the mobility of the enantiomers is initially cationic with effective mobilities between 15 and 20 mobility

units. As the ODMS concentration is increased, the mobilities approach zero due to the ionic strength related depression of the mobilities without the effective mobilities becoming anionic. The separation selectivity curves gradually increase without appearing to approach any limiting value (e.g., naphthylethylamine) or approaching a limiting value of $\alpha < 1$ (e.g., chlophedianol and salbutamol). Representative electropherograms obtained for the low pH separation of some of the weakly complexing weak bases are included in Figure 31.

A strongly binding base is one whose low pH mobility is cationic at low ODMS concentrations and anionic at high ODMS concentrations. Figure 32 shows the mobility and separation selectivity curves for three typically, strongly binding weak bases. Noteworthy is the mobility curve obtained for piperoxan. One enantiomer of piperoxan migrates cationically and the other anionically for the entire ODMS concentration range used in this study. The high peak resolution observed for the separation of piperoxan into its respective enantiomers is very much similar to that found in similar studies using the β -CD analog to ODMS indicating that dimethyl SiSCD's present a highly enantioselective environment to piperoxan enantiomers.

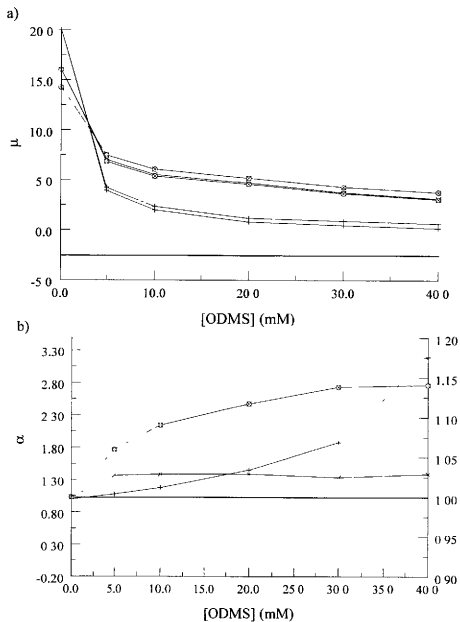


Figure 30. Mobility a) and separation selectivity b) curves for B33 (+), B14 (x) and B45 (o) in pH 2.5 aqueous BGE. For b) B33 (+) is read from the left axis; B14 (x) and B45 (o) are read from the right axis. Mobility units are $10^{-5} \text{ cm}^2 \text{ V}^{-1} \text{ s}^{-1}$.

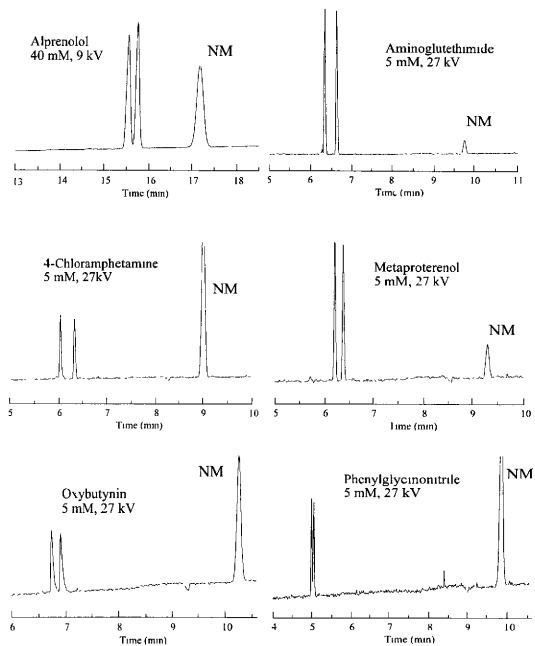


Figure 31. Capillary electrophoretic separations of some weakly-binding bases using ODMS as chiral resolving agent in pH 2.5 aqueous BGE. NM is nitromethane.

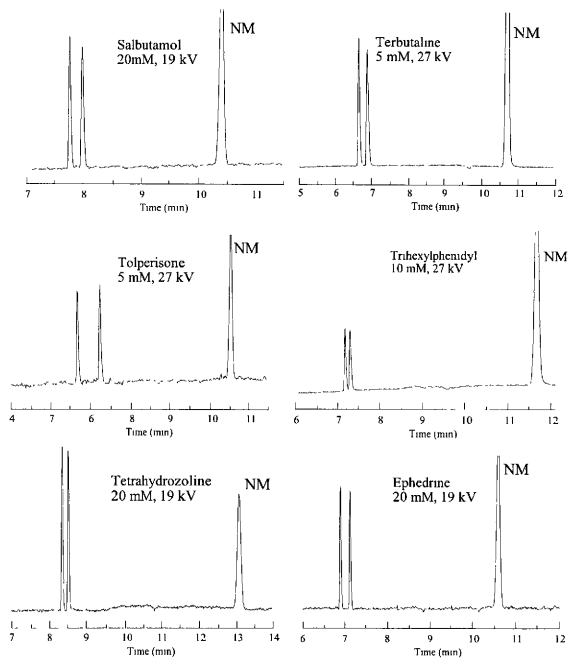


Figure 31. Continued

For the strongly binding bases, separation selectivities increase asymptotically to infinity while both enantiomers migrate cationically. As the mobility of the slower enantiomer approaches zero mobility, there is a discontinuity in separation selectivity. For strongly binding enantiomers, peak resolution increases greatly when the mobility of one of the enantiomers approaches zero. Representative electropherograms obtained for the separation of some of the strongly binding weak bases are included in Figure 33.

There are far fewer enantiomers for which favorable separation selectivity was found in the high pH BGE than in the low pH BGE. However, the utility of ODMS as a chiral selector in high pH BGE's cannot be neglected based strictly on this fact. To the contrary, while only 14 of the 36 enantiomers screened for separation selectivity in the high pH BGE showed measurable selectivity, six of the fourteen had dramatically different separation selectivity patterns in the high pH versus low pH BGE including diltiazem, which showed no separation selectivity in the low pH BGE. Thus, diltiazem constitutes the lone desionoselective separation observed for the entire set of chiral separations presented. Representative electropherograms obtained for the separation of some weak base enantiomers in the high pH BGE are included in Figure 34.

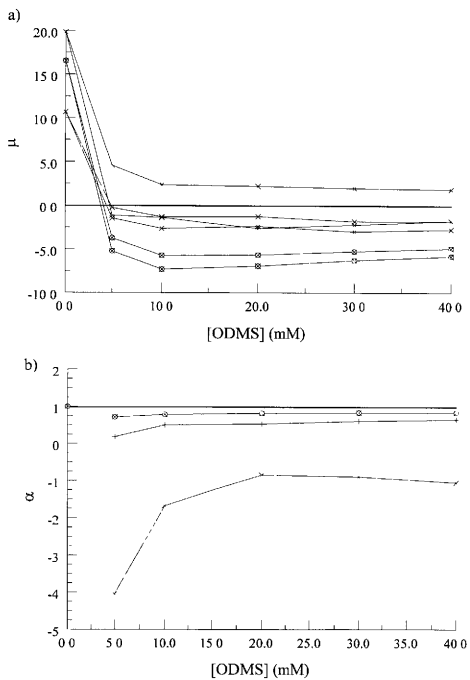


Figure 32. Mobility a) and separation selectivity b) curves for B18 (+), B38 (x) and B42

(o) in pH 2.5 aqueous BGE. Mobility units are $10^{-5} \text{ cm}^2 \text{ V}^{-1} \text{ s}^{-1}$.

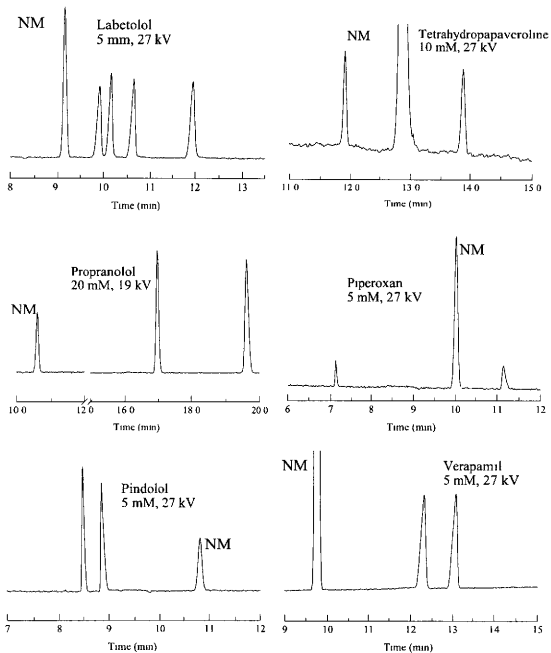


Figure 33. Capillary electrophoretic separations of some strongly-binding bases using ODMS as chiral resolving agent in pH 2.5 aqueous BGE. NM is nitromethane.

3.3.2 Weakly Acidic Enantiomer Separations in Aqueous BGE's

Use of ODMS for the separation of a set of thirteen weak acid enantiomers yielded a total of eight separations with $\alpha > 1$. The mobilities of the weak acid analytes in the ODMS-free BGE's are initially zero in the low pH BGE and ranged from -25 to -15 mobility units in the high pH BGE, respectively, as expected for weakly acidic compounds. At low pH, the acids become increasingly anionic with increasing ODMS concentration. Separation selectivities observed for the low pH weak acid separations pass through a maximum at low ODMS concentration and are generally between 1.01 and 1.1, with trans-2-phenyl-1-cyclopropanecarboxylic acid (TPCA) showing exceptional separation selectivity at 1.4. Baseline resolution was observed for six of the eight analytes with $\alpha > 1$ because of good β values. Figure 35 shows typical mobility and separation selectivity plots for some of the weakly acidic enantiomers in the low pH BGE.

At high pH, the trend in the mobility is opposite from that observed in the low pH separations. The anionic effective mobility of the enantiomers are high at low ODMS concentration and become lower as the ODMS concentration is increased due to both complexation with ODMS and the mobility suppressing effects of the increasing ionic strength. Separation selectivities were poor resulting in a lack of separation despite comparable β values to those seen in the low pH measurements. The only exception was fenoprofen with $\alpha = 1.02$ and baseline resolution at 40 mM ODMS.

While the solubility of the weak acid enantiomers was certainly better in the high pH BGE, separation selectivity was observed only for fenoprofen enantiomers. It is interesting to note the structural similarities between fenoprofen and ketoprofen

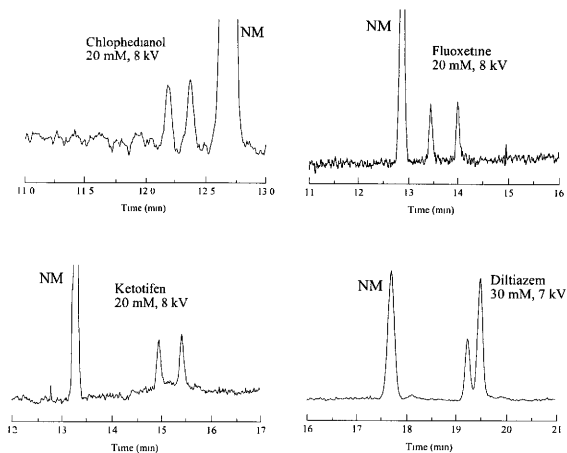


Figure 34. Capillary electrophoretic separations of weakly basic analytes using ODMS as chiral resolving agent in pH 9.5 aqueous BGE. NM is DMSO.

enantiomers and that, in the high pH BGE, the ketoprofen enantiomers showed no separation even though both possessed comparable β values, -1.75 and -1.9, respectively. Also, it has been stated that the dimethylated SiSCD's present a hydrophobic surface to complexing enantiomers and thus, have a greater tendency to exhibit weak hydrophobic interactions to bring about enantioselectivity. If this is true then, one might expect a more negative effective mobility for a hydrophobic enantiomer like 2-phenylpropionic acid as compared to the more hydrophilic mandelic acid when in fact, the opposite is observed. Finally, ethosuximide and α -methyl- α -phenylsuccinimide differ at the α position with ethosuximide possessing an ethyl substituent and α -methyl- α -phenylsuccinimide possessing a phenyl substituent. This difference is significant enough to cause ethosuximide to show no measurable separation selectivity at any ODMS concentration in contrast to the $\alpha = 1.14$ for α -methyl- α -phenylsuccinimide in 20 mM ODMS in low pH BGE. Representative electropherograms obtained for the separation of other weak acid enantiomers in the low pH BGE are included in Figure 36.

3.3.3 Nonionic Enantiomer Separations in Aqueous BGE's

Investigation into the potential use of ODMS as a chiral resolving agent for the enantioseparation of neutral compounds resulted in measurable selectivity for five of eighteen nonionic enantiomers, mostly aromatic alcohols, three of which showed sufficient separation selectivity at the concentrations used to be baseline resolved. The anionic mobilities of the non-charged enantiomers increased almost monotonically with increasing ODMS concentration. The selectivity plots resemble those obtained for the weak acid enantiomer separations at low pH.

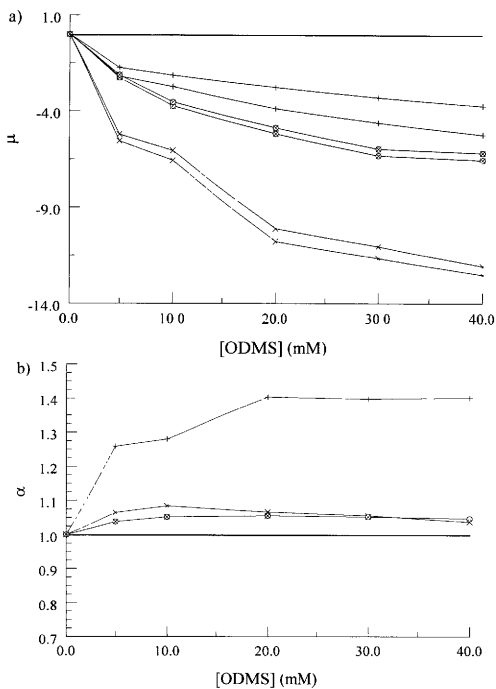


Figure 35. Mobility a) and separation selectivity b) curves for A02 (+), A22 (x) and A31 (o) in pH 2.5 aqueous BGE. Mobility units are $10^{-5} \text{ cm}^2 \text{ V}^{-1} \text{ s}^{-1}$.

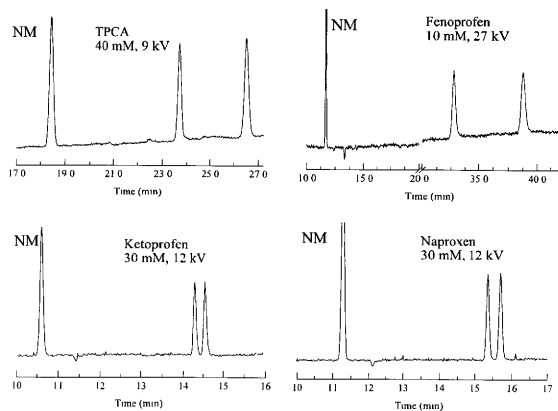


Figure 36. Capillary electrophoretic separations of weakly acidic analytes using ODMS as chiral resolving agent in pH 2.5 aqueous BGE. NM is nitromethane.

The sensitivity of the enantiorecognition mechanism becomes apparent with the comparison of the separations of ethylmandelate and methylmandelate. While ethylmandelate was separated, methylmandelate was not. The very weakly complexed neutral compounds possessed only a very slight anionic mobility in the range of -2.0 to -2.4 mobility units at the highest ODMS concentration used, resulting in exceptionally poor β values ranging from -7.9 to -12. Others that showed no separation selectivity were as far away from the ideal -1 value as -250! The tendency for very weak complexation of nonionic enantiomers was also seen with HDMS, where higher chiral resolving agent concentrations lead to more successful separations. Representative electropherograms obtained for the separation of non-ionic enantiomers in the low pH BGE are included in Figure 37.

Tables 1 and 2 list the effective mobilities of the less mobile enantiomer (μ_2^{eff}), the separation selectivity (α), the corresponding normalized electroosmotic flow (β), the peak resolution and the injector-to-detector potential drop (U) values in the low and high pH BGE's, respectively. N/A indicates that the aforementioned values could not be calculated due to either overlap with non-comigrating system peaks or comigration of an enantiomer peak with the neutral marker.

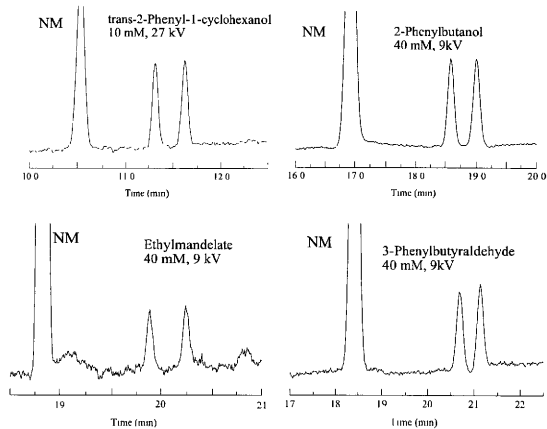


Figure 37. Capillary electrophoretic separations of non-ionic analytes using ODMS as chiral resolving agent in pH 2.5 aqueous BGE. NM is nitromethane.

Table 1.

Electrophoretic data for weakly basic, acidic and non-ionic analytes in pH 2.5 aqueous BGE (μ units are $10^{-5} \text{ cm}^2 \text{ V}^{-1} \text{ s}^{-1}$).

Analyte	0 mM	5 mM (U = 22.9 kV)				10 mM (U = 22.9 kV)			
	μ	μ^{eff}	α	β	Rs	μ^{eff}	α	β	Rs
B02	15.8	5.0	1.08	1.99	1.85	4.0	1.11	2.83	2.86
B03	17.3	6.4	1.15	1.89	4.57	4.8	1.21	2.32	6.96
B04	21.5	9.3	1.01	1.17	0.54	8.7	1.02	1.24	0.82
B05	22.7	11.4	1.02	0.98	0.59	9.7	1.02	1.45	0.96
B06	22.1	9.6	1.09	1.08	2.22	8.2	1.12	1.01	5.95
B08	14.4	5.8	1.01	2.04	0.36	4.4	1.02	1.59	1.00
B09	16.5	6.2	1.05	1.80	1.07	5.1	1.05	2.08	1.06
B10	14.8	7.0	1.00	1.62	0.00	5.5	1.00	1.99	0.00
B11	16.0	7.9	1.00	1.32	0.00	6.8	1.00	1.61	0.00
B13	21.4	5.5	1.16	2.22	4.66	3.6	1.23	2.92	4.37
B14	16.0	6.9	1.03	1.46	1.11	5.4	1.03	1.98	1.11
B16	18.1	5.9	1.03	1.81	1.14	4.4	1.03	2.39	1.03
B18	14.8	1.4	1.16	6.53	1.41	-3.1	0.52	-3.37	13.94
B19	17.0	6.2	1.06	1.77	1.33	5.0	1.07	2.10	1.66
B20	19.7	7.6	1.17	1.60	3.46	5.9	1.18	1.78	6.04
B21	15.7	5.9	1.02	1.76	0.66	4.6	1.04	2.27	1.38
B22	18.2	9.6	1.02	1.07	1.00	8.9	1.03	0.92	1.64
B23	15.4	-1.1	-0.21	-9.33	5.33	-2.3	0.60	-5.99	0.95
B24	13.4	-0.9	0.78	-13.24	1.56	-2.4	1.05	-4.46	1.53
		-1.1	0.71	-10.33	3.16	-2.5	1.20	-4.24	6.08
		-1.6	0.60	-7.34	7.65	-3.0	1.30	-3.53	2.47
B25	14.9	5.1	1.00	2.42	0.00	3.7	1.00	2.83	0.00
B26	18.7	4.9	1.03	2.34	0.84	3.4	1.00	3.10	0.00
B27	15.5	7.8	1.00	1.45	0.00	6.3	1.00	1.68	0.00
B28	20.1	10.6	1.01	1.31	0.19	8.6	1.01	1.24	0.57
B30	17.3	5.6	1.09	2.14	2.78	3.8	1.15	2.77	3.76
B31	15.2	4.7	1.00	2.39	0.00	3.4	1.00	3.16	0.00
B33	20.0	3.9	1.08	2.81	1.70	2.0	1.18	5.38	2.15
B34	21.4	9.6	1.05	1.16	2.24	8.3	1.06	1.26	2.56
B35	15.0	5.3	1.08	2.04	1.93	4.0	1.11	2.57	2.38
B36	15.0	5.2	1.00	2.10	0.00	4.0	1.00	2.61	0.00
B37	16.9	7.2	1.00	1.51	0.00	5.7	1.00	1.82	0.00
B38	19.8	-1.1	-4.05	-9.86	34.04	-1.4	-1.68	-10.05	17.14
B39	23.5	11.0	1.02	1.01	1.09	9.1	1.03	1.15	1.45
B41	16.8	2.3	1.25	4.46	3.66	0.2	3.43	41.46	6.41
B42	16.5	-5.2	0.71	-1.93	14.40	-7.3	0.78	-1.44	23.19

Table 1. Continued

Analyte	20 mM (U = 16.1 V/cm)				30 mM (U = 10.2 V/cm)				40 mM (U = 7.6 V/cm)			
	μ_2^{eff}	α	β	Rs	μ_2^{eff}	α	β	Rs	μ_2^{eff}	α	β	Rs
B02	2.6	1.17	5.89	2.16	2.1	1.14	9.78	1.16	1.8	1.15	10.81	1.19
B03	3.7	1.26	4.28	6.23	3.4	1.24	6.05	3.67	3.2	1.16	4.77	1.42
B04	7.6	1.02	2.13	0.81	7.2	1.02	2.90	0.66	6.8	1.02	2.97	0.63
B05	8.2	1.03	1.48	1.36	7.5	1.04	2.66	1.09	6.9	1.04	2.91	0.93
B06	7.1	1.13	1.77	5.06	6.5	1.13	3.19	3.58	6.2	1.12	3.24	3.62
B08	3.3	1.03	4.85	0.58	2.8	1.04	7.38	0.45	2.4	1.04	5.72	0.61
B09	4.3	1.08	3.73	1.69	3.8	1.09	5.42	1.29	3.2	1.11	4.80	2.73
B10	4.4	1.00	3.63	0.00	3.6	1.00	5.72	0.00	3.2	1.00	4.25	0.00
B11	5.6	1.00	2.82	0.00	4.7	1.00	4.44	0.00	3.9	1.00	3.73	0.00
B13	3.1	1.26	4.28	4.01	2.7	1.29	4.93	3.94	2.5	1.26	5.46	2.92
B14	4.6	1.03	2.91	0.79	3.7	1.02	5.62	0.42	3.1	1.03	4.34	0.37
B16	3.8	1.03	3.49	0.47	3.3	1.00	6.25	0.00	2.6	1.00	5.19	0.00
B18	-2.9	0.49	-4.60	13.91	-2.9	0.50	-7.03	9.24	-2.8	0.50	-4.86	10.38
B19	4.4	1.10	3.05	2.09	3.8	1.12	3.45	2.53	3.5	1.12	5.28	1.72
B20	5.3	1.13	2.50	2.75	4.8	1.09	2.75	1.75	4.5	1.01	4.15	0.19
B21	3.7	1.07	3.61	1.06	2.9	1.08	6.23	0.96	2.3	1.09	8.04	1.13
B22	7.3	1.04	2.35	1.33	6.4	1.05	3.09	1.03	6.0	1.05	2.29	0.14
B23	-3.1	0.73	-4.31	1.27	-3.3	0.80	-5.43	0.72	-3.3	0.83	-5.70	0.76
B24	-3.0	1.00	-4.37	0.00	-3.0	1.00	-5.67	0.00	-3.2	1.00	-5.91	0.00
	-3.0	1.16	-4.37	5.00	-3.0	1.13	-5.67	2.73	-3.2	1.11	-5.91	2.06
	-3.5	1.20	-3.78	7.73	-3.4	1.15	-5.02	3.86	-3.5	1.13	-5.33	3.24
B25	3.0	1.00	4.83	0.00	2.2	1.00	4.75	0.00	1.8	1.00	10.49	0.00
B26	2.3	1.00	7.62	0.00	2.0	1.00	8.60	0.00	1.8	1.00	10.13	0.00
B27	5.3	1.00	2.47	0.00	4.3	1.03	3.05	0.73	3.4	1.07	3.93	1.25
B28	7.6	1.00	1.63	0.19	6.6	1.00	2.60	0.00	6.1	1.00	2.61	0.00
B30	2.7	1.28	4.92	7.19	1.9	1.34	9.22	2.67	1.3	1.35	11.00	2.75
B31	2.6	1.00	4.95	0.00	2.0	1.00	8.81	0.00	1.5	1.00	9.08	0.00
B33	0.8	1.45	25.48	2.03	0.5	1.88	36.11	2.49	0.2	3.20	77.37	2.62
B34	7.5	1.07	2.77	1.94	6.7	1.07	2.71	2.15	6.4	1.07	2.54	1.94
B35	3.0	1.16	5.87	1.66	2.0	1.16	9.07	1.82	1.8	1.17	9.21	1.57
B36	2.9	1.00	6.29	0.00	2.2	1.00	9.32	0.00	2.0	1.00	8.56	0.00
B37	4.5	1.00	4.05	0.00	3.8	1.00	5.45	0.00	2.7	1.00	6.23	0.00
B38	-2.6	-0.84	-7.03	27.75	-2.2	-0.89	-9.24	22.97	-1.8	-1.04	-9.70	21.58
B39	8.4	1.04	2.19	1.36	7.6	1.04	2.69	1.30	7.0	1.04	2.39	1.31
B41	-0.8	0.32	-18.24	4.69	-1.3	0.63	-10.41	2.88	-1.6	0.74	-8.65	3.02
B42	-6.9	0.82	-2.16	14.32	-6.3	0.83	-3.21	8.47	-5.8	0.84	-2.88	4.74

Table 1. Continued

Analyte	0 mM					5 mM (U = 22.9 V/cm)					10 mM (U = 22.9 V/cm)				
	μ	μ_2^{eff}	α	β	Rs	μ_2^{eff}	α	β	Rs	μ_2^{eff}	α	β	Rs		
B43	14.1	3.0	1.03	3.69	0.51	1.3	1.09	4.92	0.77						
B45	14.3	7.1	1.06	1.63	1.52	5.6	1.09	1.58	3.63						
B46	16.0	6.5	1.00	1.58	0.00	5.2	1.00	1.67	0.00						
B47	16.5	5.9	1.10	1.82	2.32	4.0	1.16	2.15	5.42						
B49	15.0	0.9	2.87	13.04	8.00	-0.6	-1.12	-13.56	17.38						
B51	17.2	5.5	1.27	2.01	7.26	4.0	1.39	2.17	12.68						
B53	13.2	6.1	1.03	1.77	0.77	5.2	1.04	1.75	1.58						
B54	11.3	-2.9	0.81	-4.08	3.35	-3.6	0.88	-2.15	10.18						
B57	10.4	4.2	1.00	2.82	0.00	3.6	1.00	2.53	0.00						
B58	20.8	8.9	1.05	1.23	1.60	6.3	1.06	1.01	3.12						
B60	18.4	10.8	1.07	2.07	0.95	8.4	1.09	0.82	4.43						
B61	20.8	11.3	1.00	1.36	0.00	6.1	1.01	1.14	0.38						
A02	-0.3	-1.7	1.26	-8.89	2.46	-2.1	1.28	-5.01	6.26						
A03	0.0	-0.5	1.00	-28.81	0.00	-0.5	1.10	-23.52	0.47						
A09	0.0			N/A				N/A							
A22	-0.6	-5.2	1.06	-3.03	3.06	-6.0	1.08	-1.53	9.37						
A23	insoluble	-1.0	1.00	-11.31	0.00	-1.7	1.05	-6.00	0.62						
A27	-0.8	-1.7	1.04	-7.18	0.47	-2.8	1.05	-3.62	1.33						
A28	-0.2	-3.2	1.00	-3.97	0.00	-4.0	1.00	-2.45	0.06						
A31	insoluble	-2.1	1.06	-6.13	1.23	-3.5	1.06	-2.84	3.16						
A36	-0.4	-0.9	1.00	-15.08	0.00	-1.3	1.00	-7.47	0.00						
N02	0.0	-0.3	1.10	-34.72	0.29	-0.6	1.21	-20.44	1.00						
N10	0.0	-0.2	1.00	-66.37	0.00	-0.3	1.00	-38.14	0.00						
N15	0.0			N/A		-0.3	1.00	-37.18	0.00						
N19	0.0			N/A				N/A							
N20	0.0	-0.4	1.00	-30.79	0.00	-0.7	1.00	-17.28	0.00						
N21	0.0	-0.4	1.00	-33.73	0.00	-0.7	1.00	-17.17	0.00						
N22	0.0	-0.4	1.00	-30.67	0.00	-0.7	1.15	-18.02	0.84						
N24	0.0	-0.2	1.00	-59.36	0.00	-0.3	1.00	-34.65	0.00						
N25	0.0	-0.4	1.00	-27.26	0.00	-0.8	1.00	-14.63	0.00						
N26	0.0	-0.3	1.00	-36.59	0.00	-0.6	1.00	-18.79	0.00						
N27	0.0	-0.3	1.00	-38.68	0.00	-0.5	1.02	-20.95	0.10						
N30	0.0	-0.4	1.35	-29.11	1.09	-0.7	1.34	-14.11	2.53						
N34	0.0	-0.4	1.00	-34.26	0.00	-0.6	1.00	-16.91	0.00						
N36	0.0	-0.4	1.00	-31.57	0.00	-0.7	1.00	-15.62	0.00						
N38	0.0	-0.3	1.00	-31.57	0.00	-0.6	1.00	-15.62	0.00						
N39	0.0	-0.3	1.00	-44.72	0.00	-0.5	1.00	-18.73	0.00						
N40	0.0	-0.6	1.00	-40.62	0.00	-1.1	1.00	-19.60	0.00						

Table 1. Continued

Analyte	20 mM (U = 16.1 kV)				30 mM (U = 10.2 kV)				40 mM (U = 7.6 kV)			
	μ_2^{eff}	α	β	R_s	μ_2^{eff}	α	β	R_s	μ_2^{eff}	α	β	R_s
B43	0.6	1.11	14.37	0.60	-0.4	1.00	-33.18	0.00	-0.4	1.00	-30.36	0.00
B45	4.7	1.12	3.28	2.89	3.8	1.14	5.32	2.49	3.3	1.14	4.89	2.19
B46	4.6	1.00	3.33	0.00	4.0	1.00	3.26	0.00	3.7	1.00	4.43	0.00
B47	2.9	1.25	5.19	5.74	2.0	1.29	10.23	2.94	1.5	1.37	10.53	3.36
B49	-1.7	0.30	-8.75	8.76	-2.1	0.51	-9.64	6.75	-2.3	0.63	-5.80	6.77
B51	3.3	1.47	4.55	7.47	2.8	1.49	5.79	8.67	2.4	1.52	7.57	5.90
B53	4.2	1.05	3.62	1.18	3.4	1.06	3.84	1.07	2.7	1.07	5.08	0.79
B54	-4.5	0.90	-3.32	3.64	-4.8	0.92	-4.20	1.80	-4.6	0.93	-3.89	2.48
B57	1.7	1.00	8.96	0.00	1.2	1.00	13.71	0.00	0.7	1.00	25.03	0.00
B58	6.0	1.06	2.03	2.07	5.5	1.06	3.78	1.45	5.0	1.06	3.54	1.40
B60	7.4	1.10	2.03	3.72	6.5	1.11	3.16	3.19	6.1	1.11	2.89	2.93
B61	5.1	1.00	2.91	0.00	4.5	1.00	4.61	0.00	4.1	1.00	4.25	0.00
A02	-2.8	1.40	-4.10	10.81	-3.3	1.40	-3.20	11.53	-3.7	1.40	-4.78	9.07
A03	-0.9	1.14	-12.98	0.91	-1.1	1.12	-8.96	1.02	-1.5	1.12	-13.55	0.73
A09	-0.1	1.00	-94.34	0.00	-0.2	1.00	-57.45	0.00	-0.3	1.00	-58.57	0.00
A22	-10.1	1.07	-2.41	1.83	-11.0	1.06	-2.06	4.91	-12.1	1.04	-1.50	5.11
A23	-2.8	1.06	-4.33	1.76	-3.5	1.05	-6.49	0.64	-4.1	1.05	-3.13	1.89
A27	-4.4	1.06	-2.78	2.66	-5.6	1.05	-4.02	1.84	-6.7	1.05	-2.70	2.31
A28	-4.1	1.01	-3.00	0.44	-4.2	1.02	-2.50	0.60	-4.5	1.02	-2.79	0.65
A31	-4.9	1.06	-2.51	5.82	-6.0	1.06	-3.74	2.13	-6.2	1.06	-2.98	1.78
A36	-2.2	1.00	-5.17	0.00	-2.5	1.01	-4.06	0.33	-2.9	1.02	-4.26	0.43
N02	-1.1	1.23	-10.83	2.05	-1.3	1.23	-19.74	1.41	-1.8	1.22	-11.10	1.95
N10	-0.6	1.04	-21.10	0.19	-0.8	1.11	-12.76	0.60	-1.1	1.09	-18.31	0.47
N15	-0.6	1.00	-20.42	0.00	-0.8	1.00	-12.33	0.00	-1.1	1.00	-17.89	0.00
N19	-0.1	1.00	-135.46	0.00	-0.1	1.00	-70.79	0.00	-0.2	1.00	-116.85	0.00
N20	-1.3	1.00	-9.85	0.00	-1.8	1.00	-8.82	0.00	-2.2	1.00	-8.72	0.00
N21	-1.1	1.08	-11.45	0.62	-1.6	1.00	-6.16	0.00	-2.2	1.00	-8.64	0.00
N22	-1.1	1.17	-12.08	1.38	-1.5	1.17	-20.55	0.71	-2.0	1.17	-9.47	1.44
N24	-0.5	1.00	-25.53	0.00	-0.7	1.00	-39.83	0.00	-0.9	1.00	-14.12	0.00
N25	-1.3	1.00	-9.78	0.00	-1.7	1.00	-8.23	0.00	-2.2	1.00	-5.78	0.00
N26	-1.0	1.00	-12.66	0.00	-1.2	1.00	-16.29	0.00	-1.8	1.00	-9.81	0.00
N27	-0.8	1.11	-14.60	0.63	-1.1	1.06	-15.87	0.45	-1.5	1.10	-12.20	0.33
N30	-1.3	1.39	-9.52	3.93	-2.0	1.32	-9.06	3.94	-2.4	1.37	-7.85	2.00
N34	-1.1	1.00	-11.64	0.00	-1.2	1.00	-13.24	0.00	-1.8	1.00	-10.51	0.00
N36	-1.1	1.00	-11.23	0.00	-1.5	1.00	-18.19	0.00	-1.9	1.00	-6.16	0.00
N38	-0.9	1.00	-11.23	0.00	-1.3	1.00	-18.19	0.00	-1.7	1.00	-6.16	0.00
N39	-0.9	1.00	-13.02	0.00	-1.2	1.00	-19.59	0.00	-1.6	1.00	-6.71	0.00
N40	-1.8	1.00	-23.90	0.00	-2.2	1.00	-21.52	0.00	-2.6	1.00	-7.18	0.00

Table 2.

Electrophoretic data for weakly basic, acidic and non-ionic analytes in pH 9.5 aqueous BGE (μ units are $10^{-5} \text{ cm}^2 \text{ V}^{-1} \text{ s}^{-1}$)

Analyte	0 mM					5 mM (U = 8.5 kV)				10 mM (U = 6.8 kV)			
	μ	μ_2^{eff}	α	β	Rs	μ_2^{eff}	α	β	Rs	μ_2^{eff}	α	β	Rs
B02	11.2	4.0	1.04	12.33	0.37	3.3	1.08	11.68	0.67				
B04	14.5	7.1	1.00	6.90	0.00	5.5	1.00	7.04	0.00				
B06	6.8	4.2	1.09	11.68	0.61	2.2	1.12	18.04	0.52				
B08	10.0	4.1	1.00	12.11	0.00	3.5	1.00	10.93	0.00				
B09	11.3					3.5	1.00	11.23	0.00				
B10	0.7												
B11	1.3	0.4	1.00	130.98	0.00	0.8	1.00	45.58	0.00				
B13	14.8	4.4	1.14	10.30	1.45	3.8	1.19	10.02	1.63				
B14	5.9	2.7	1.05	17.33	0.36	1.2	1.27	31.73	0.93				
B18	10.7	-1.5	0.18	-29.70	2.51	-2.6	0.50	-14.89	2.54				
B19	11.2	4.8	1.00	9.57	0.00	3.3	1.00	11.90	0.00				
B20	18.2	8.3	1.00	5.57	0.00	6.3	1.00	6.25	0.00				
B22	0.0					-0.7	1.00	-59.45	0.00				
B23	1.6	-1.3	1.00	-35.17	0.00	-2.9	0.85	-13.63	1.28				
B25	14.1	5.4	1.00	9.01	0.00	3.4	1.00	11.46	0.00				
B26	4.0	0.9	1.00	56.22	0.00	-1.1	1.00	-36.33	0.00				
B28	17.9	10.4	1.00	4.67	0.00	8.0	1.00	4.88	0.00				
B30	0.0	-1.1	1.00	-45.14	0.00	-4.6	1.00	-8.64	0.00				
B31	8.4	3.9	1.00	12.49	0.00	1.6	1.00	24.50	0.00				
B33	8.2	0.7	1.00	61.53	0.00								
B34	6.9	2.6	1.00	16.73	0.00	2.3	1.00	16.97	0.00				
B36	25.0	12.5	1.00	3.50	0.00	12.7	1.00	3.13	0.00				
B37	9.3	5.4	1.00	9.02	0.00	2.7	1.00	14.46	0.00				
B38	2.3	0.8	1.00	62.71	0.00	-1.0	0.41	-37.74	1.67				
B39	0.0					-0.7	1.00	-59.76	0.00				
B41	10.8					-0.4	1.00	-87.74	0.00				
B42	9.7	-3.7	0.67	-13.12	3.28	-4.9	0.79	-7.96	3.87				
B43	6.9	1.9	1.00	21.05	0.00	0.4	1.00	90.88	0.00				
B45	6.0	2.6	1.00	18.58	0.00	0.8	1.21	49.22	0.51				
B46	0.2												
B47	2.4					-1.4	1.00	-28.55	0.00				
B51	5.4	1.2	1.38	41.80	0.95	1.6	1.37	24.69	1.52				
B57	0.4					-0.8	1.00	-50.87	0.00				
B58	19.2	8.3	1.04	4.96	0.83	7.3	1.06	5.47	1.04				
B60	13.7	5.2	1.08	9.26	0.98	5.9	1.09	6.78	1.21				
B61	3.5					0.7	1.00	58.31	0.00				

Table 2. Continued

Analyte	20 mM (U = 6.8 kV)				30 mM (U = 5.9 kV)				40 mM (U = 7.6 kV)			
	μ^{eff}	α	β	Rs	μ^{eff}	α	β	Rs	μ^{eff}	α	β	Rs
B02	0.8	1.07	35.66	0.25	N/A				-0.1	1.00	-207.05	0.00
B04	3.2	1.00	8.99	0.00	3.1	1.00	9.05	0.00	2.8	1.00	6.56	0.00
B06	1.5	1.14	19.68	0.53	1.2	1.18	22.89	0.65	1.1	1.18	17.08	0.59
B08	1.2	1.00	23.85	0.00	0.9	1.00	30.20	0.00	0.7	1.00	27.50	0.00
B09	2.6	1.00	11.01	0.00	2.5	1.00	9.15	0.00	1.8	1.00	10.06	0.00
B10	-0.8	1.00	-37.60	0.00	-1.3	1.00	-20.36	0.00	-1.5	1.00	-11.98	0.00
B11	-0.8	1.00	-34.73	0.00	-1.5	1.00	-17.85	0.00	-1.7	1.00	-10.36	0.00
B13	1.7	1.34	17.07	1.87	1.4	1.34	18.51	1.91	1.3	1.31	14.04	1.93
B14	0.7	1.63	40.10	1.92	-0.4	-1.04	-66.35	2.76	-1.0	0.10	-18.80	5.72
B18	-2.4	0.53	-12.29	4.30	-3.0	0.61	-7.58	4.57	-2.7	0.65	-6.57	3.38
B19	2.7	1.00	10.63	0.00	2.9	1.00	8.61	0.00	2.1	1.00	8.50	0.00
B20	4.5	1.00	6.33	0.00	4.8	1.00	5.16	0.00	3.8	1.00	4.66	0.00
B22	-1.0	1.00	-27.17	0.00	-1.7	1.00	-16.68	0.00	-2.0	1.00	-9.27	0.00
B23	-3.9	0.80	-7.19	2.86	-5.5	0.80	-4.19	5.80	-6.0	0.77	-3.05	10.35
B25	2.2	1.00	12.76	0.00	2.1	1.00	11.18	0.00	1.5	1.00	11.86	0.00
B26	-1.4	1.00	-19.58	0.00	-2.8	1.00	-10.41	0.00	-2.5	1.00	-7.41	0.00
B28	5.9	1.00	4.72	0.00	5.7	1.00	4.88	0.00	4.8	1.00	3.81	0.00
B30	-3.0	1.00	-9.47	0.00	-4.4	1.00	-5.41	0.00	-3.8	1.00	-4.87	0.00
B31	1.3	1.00	21.76	0.00	0.7	1.00	31.61	0.00	0.6	1.00	31.81	0.00
B33	-1.0	0.87	-27.72	0.40	-2.4	0.94	-9.36	0.53	-2.7	0.96	-7.08	0.59
B34	2.4	1.00	11.20	0.00	1.5	1.00	15.15	0.00	1.1	1.00	17.71	0.00
B36	N/A				2.3	1.00	9.96	0.00	0.7	1.00	28.35	0.00
B37	2.2	1.00	15.18	0.00	1.3	1.00	18.40	0.00	0.4	1.00	44.45	0.00
B38	-1.6	0.57	-20.32	2.39	-2.2	0.73	-10.60	2.49	-2.2	0.83	-8.53	2.17
B39	-1.0	1.00	-29.00	0.00	-1.6	1.00	-14.60	0.00	-1.7	1.00	-11.09	0.00
B41	-1.1	0.72	-24.94	1.36	-2.1	0.87	-11.14	1.29	-2.2	0.91	-8.52	1.18
B42	-4.8	0.83	-5.79	3.97	-5.4	0.86	-4.24	4.14	-4.7	0.88	-4.03	3.93
B43	-0.5	1.00	-55.58	0.00	-1.5	1.00	-14.91	0.00	-2.2	1.00	-8.56	0.00
B45	0.6	1.35	45.36	0.62	N/A				-1.0	0.87	-18.68	0.57
B46	-0.4	1.00	-66.13	0.00	-0.8	1.00	-27.23	0.00	-1.0	1.00	-18.30	0.00
B47	-1.5	1.00	-18.56	0.00	-1.8	1.00	-12.48	0.00	-2.2	1.00	-8.40	0.00
B51	1.5	1.46	22.93	1.79	0.4	2.12	57.09	1.98	-0.3	1.00	-55.88	0.00
B57	-1.5	0.87	-18.25	0.88	-2.2	0.87	-10.88	1.29	-2.4	0.88	-7.64	1.65
B58	5.4	1.06	5.15	1.00	5.0	1.06	4.92	1.14	3.9	1.06	4.69	1.13
B60	4.7	1.10	5.92	1.42	3.2	1.12	7.66	1.32	3.4	1.13	5.50	1.74
B61	0.3	1.00	104.74	0.00	-2.2	1.00	-11.01	0.00	-0.8	1.00	-22.40	0.00

Table 2. Continued

Analyte	0 mM	5 mM (U = 8.5 kV)				10 mM (U = 6.8 kV)			
	μ	μ_2^{eff}	α	β	Rs	μ_2^{eff}	α	β	Rs
A02	-20.3	-20.3	1.00	-2.37	0.00	-18.8	1.00	-2.19	0.00
A03	-16.3	-14.2	1.00	-2.83	0.00	-14.4	1.00	-2.81	0.00
A04	-15.9	-16.7	1.00	-2.90	0.00	-15.6	1.00	-2.63	0.00
A09	-8.4	-10.2	1.00	-3.96	0.00	-10.4	1.00	-3.90	0.00
A16	-12.9	-12.5	1.00	-3.23	0.00	-13.4	1.00	-2.99	0.00
A22	-16.8	-16.7	1.00	-2.89	0.00	-15.5	1.00	-2.65	0.00
A23	-16.9	-16.6	1.00	-2.91	0.00	-15.3	1.00	-2.69	0.00
A26	-17.1	-16.9	1.00	-2.87	0.00	-15.8	1.00	-2.61	0.00
A27	-16.3	-16.0	1.00	-3.03	0.00	-14.7	1.00	-2.79	0.00
A28	-22.5	-20.5	1.00	-2.20	0.00	-20.6	1.00	-1.96	0.00
A30	-17.7	-17.0	1.01	-2.84	-0.57	-16.0	1.01	-2.54	-0.62
A31	-17.4	-17.2	1.00	-2.83	0.00	-16.3	1.00	-2.51	0.00
A36	-22.0	-21.0	1.00	-2.32	0.00	-19.4	1.00	-2.10	0.00
N02	0.0	-0.3	1.00	-151.00	0.00	-0.7	1.00	-59.74	0.00
N10	0.0			N/A		-0.4	1.00	-102.75	0.00
N15	0.0			N/A				N/A	
N19	0.0			N/A				N/A	
N20	0.0			N/A		-0.7	1.00	-54.53	0.00
N21	0.0	-0.4	1.00	-126.88	0.00	-0.8	1.00	-52.29	0.00
N22	0.0			N/A				N/A	
N24	0.0			N/A		-0.4	1.00	-109.92	0.00
N25	0.0	-0.4	1.00	-118.32	0.00	-0.8	1.00	-47.65	0.00
N26	0.0	-0.3	1.00	-154.85	0.00	-0.7	1.00	-60.81	0.00
N30	0.0			N/A		-0.8	1.32	-51.93	-0.62
N34	0.0	-0.3	1.00	-149.98	0.00	-0.7	1.00	-63.49	0.00
N36	0.0	-0.4	1.00	-133.73	0.00	-0.7	1.00	-60.72	0.00
N38	0.0	-0.3	1.00	-133.73	0.00	-0.6	1.00	-60.72	0.00
N39	0.0			N/A		-0.5	1.00	-70.80	0.00
N40	0.0			N/A		-1.0	1.00	-87.26	0.00

Table 2. Continued

Analyte	20 mM (U = 6.8 kV)				30 mM (U = 5.9 kV)				40 mM (U = 7.6 kV)			
	μ^{eff}	α	β	Rs	μ^{eff}	α	β	Rs	μ^{eff}	α	β	Rs
A02	-15.6	1.00	-1.96	0.00	-16.4	1.00	-1.68	0.00	-14.0	1.00	-1.56	0.00
A03	-14.2	1.00	-2.15	0.00	-13.7	1.00	-2.00	0.00	-11.9	1.00	-1.80	0.00
A04	-13.7	1.00	-2.22	0.00	-14.9	1.00	-1.81	0.00	-12.9	1.00	-1.67	0.00
A09	-11.6	1.00	-2.59	0.00	-9.4	1.00	-2.85	0.00	-10.0	1.00	-1.90	0.00
A16	-11.7	1.00	-2.57	0.00	-11.9	1.00	-2.28	0.00	-10.5	1.00	-1.80	0.00
A22	-13.2	1.01	-2.27	0.47	-14.0	1.01	-1.87	1.07	-12.2	1.02	-1.75	1.64
A23	-12.6	1.00	-2.37	0.00	-13.0	1.00	-1.89	0.00	-11.1	1.00	-1.90	0.00
A26	-13.5	1.00	-2.20	0.00	-14.1	1.00	-1.62	0.00	-12.4	1.00	-1.72	0.00
A27	-12.4	1.00	-2.40	0.00	-13.0	1.00	-2.07	0.00	-11.1	1.00	-1.90	0.00
A28	-16.7	1.00	-1.77	0.00	-17.3	1.00	-1.49	0.00	-14.5	1.00	-1.58	0.00
A30	-13.0	1.01	-2.26	0.55	-13.1	1.01	-1.63	-1.09	-11.4	1.01	-1.87	0.97
A31	-13.3	1.00	-2.20	0.00	-13.7	1.00	-1.58	0.00	-11.7	1.00	-1.80	0.00
A36	-16.0	1.00	-1.81	0.00	-16.6	1.00	-1.42	0.00	-13.9	1.00	-1.56	0.00
N02	-1.0	1.18	-30.12	0.60	-1.5	1.19	-12.97	1.31	-1.8	1.19	-9.78	1.91
N10	-0.6	1.00	-47.23	0.00	-1.1	1.00	-18.18	0.00	-1.2	1.07	-15.13	0.43
N15	-0.6	1.00	-46.70	0.00	-1.0	1.00	-18.29	0.00	-1.2	1.00	-14.46	0.00
N19		N/A			-0.3	1.00	-68.09	0.00	-0.4	1.00	-44.65	0.00
N20	-1.2	1.00	-24.69	0.00	-2.1	1.00	-9.49	0.00	-2.1	1.00	-8.27	0.00
N21	-1.1	1.00	-24.94	0.00	-1.9	1.00	-8.85	0.00	-2.1	1.00	-8.25	0.00
N22	-0.9	1.00	-31.29	0.00	-1.5	1.05	-16.46	0.31	-1.6	1.07	-14.09	0.51
N24	-0.5	1.00	-56.03	0.00	-0.9	1.00	-17.14	0.00	-1.0	1.00	-21.78	0.00
N25	-1.2	1.00	-24.37	0.00	-2.1	1.00	-11.74	0.00	-2.2	1.00	-10.04	0.00
N26	-1.0	1.00	-31.64	0.00	-1.6	1.00	-10.00	0.00	-1.7	1.00	-10.75	0.00
N30	-1.2	1.34	-24.16	1.67	-2.2	1.35	-8.52	3.61	-2.3	1.34	-8.24	4.44
N34	-1.0	1.00	-29.00	0.00	-1.8	1.00	-9.48	0.00	-1.9	1.00	-9.95	0.00
N36	-1.0	1.00	-28.25	0.00	-1.7	1.00	-9.89	0.00	-1.9	1.00	-10.08	0.00
N38	-0.9	1.00	-28.25	0.00	-1.6	1.00	-9.89	0.00	-1.7	1.00	-10.08	0.00
N39	-0.7	1.00	-32.13	0.00	-1.2	1.00	-11.72	0.00	-1.4	1.00	-11.01	0.00
N40	-1.5	1.00	-40.72	0.00	-2.6	1.00	-16.80	0.00	-2.6	1.00	-13.87	0.00

3.4 Weakly Basic Enantiomer Separations in Methanolic BGE's

Several advantages exist in the use of non-aqueous BGE's as compared to aqueous ones. Non-aqueous CE (NACE) allows for separation of analytes with low water solubility. Some NACE solvents have low viscosity and low conductivity, which permits the use of higher potentials. Commonly used NACE solvents include DMSO, N-methylformamide (NMF), N,N-dimethylformamide (DMF) and propylene carbonate (PC) as well as methanol (MeOH) and acetonitrile (ACN). Some, such as DMSO, NMF, DMF, and PC have high UV cut-off values relative to the others. Since the solubility of most SiSCD's, including ODMS is adequate in methanol, this is the solvent of choice for NACE.

Study of the use of ODMS as a chiral resolving agent in an acidic non-aqueous BGE was carried out using a set of 34 weakly basic enantiomers. Table 3 lists the effective mobilities of the less mobile enantiomer (μ_2^{eff}), the separation selectivity(α), the corresponding normalized electroosmotic flow mobility (β), the peak resolution and the injector-to-detector potential drop (U) values. Once the ODMS concentration was found where the effective mobility of an analyte changed from anionic to cationic, the ODMS concentration was not decreased further because it is known that lowering the ODMS concentration after the cross-over would lead to lower separation selectivities. Mobility and separation selectivity plots for some of the weak base enantiomers are shown in Figure 38.

All 34 of the weakly basic enantiomers used in the non-aqueous effective mobility measurements showed separation selectivity at one or more of the ODMS

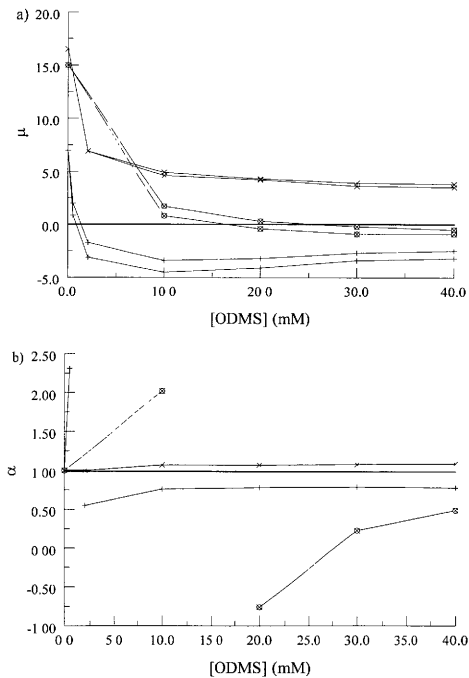


Figure 38. Mobility a) and separation selectivity b) curves for B44 (+), B14 (x) and B49

(o) in acidic methanol BGE. Mobility units are $10^{-5} \text{ cm}^2 \text{ V}^{-1} \text{ s}^{-1}$.

concentrations used. All but four were baseline resolved under the given separation conditions. A third migration behavior was observed in NACE measurements so that all the weak bases studied fell into one of three mobility patterns. The weak bases whose effective mobilities remained cationic throughout the ODMS concentration range are weakly binding and have their effective mobilities depressed toward zero by the increasing ionic strength. There is no discontinuity in the separation selectivity pattern similar to the weak base aqueous enantiomer separations. The moderately strongly binding bases migrate cationically until, at some intermediate ODMS concentration, their effective mobility becomes anionic and then is depressed back by ionic strength to a lower, though anionic value as the ODMS concentration is further increased. The third mobility pattern is similar to the pattern for strongly binding bases observed in the aqueous measurements. The effective mobility of the enantiomers becomes anionic at a low ODMS concentration, then rapidly decreases at the higher ODMS concentrations due to increasing ionic strength. A discontinuity is observed in the separation selectivity patterns of both the moderately and strongly binding weak bases. The difference between the two is that the discontinuity occurs very early on in the ODMS concentration range for the strongly binding weak bases and at some intermediate ODMS concentration for the moderately strongly binding weak bases. Favorable β values led to good peak resolution as can be seen for several of the enantiomer separations shown in Figure 39.

The four weak bases that could not be baseline resolved included bupivacaine, bupropion, metaproterenol and piperoxan. Piperoxan was noted in section 3.3.1 for its peculiarly strong binding. In NACE, its binding is weak and the enantiomers cannot be

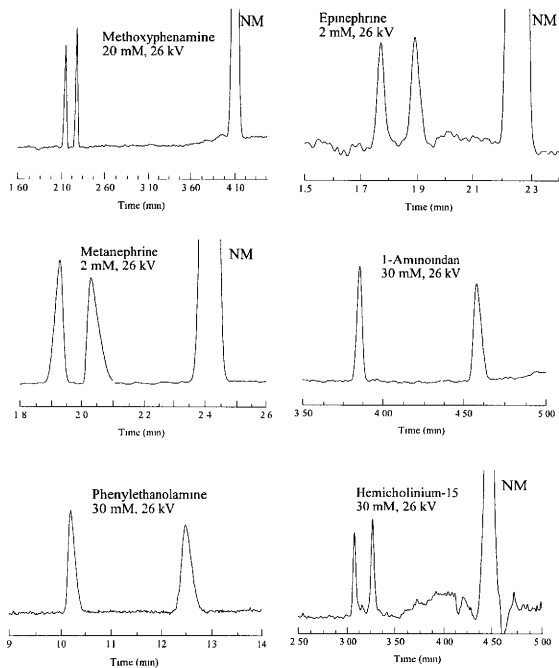


Figure 39. Capillary electrophoretic separations of weakly basic analytes using ODS as chiral resolving agent in acidic methanol BGE. NM is nitromethane.

Table 3. Continued

Analyte	2 mM				10 mM				20 mM			
	μ_2^{eff}	α	β	R_s	μ_2^{eff}	α	β	R_s	μ_2^{eff}	α	β	R_s
B02					-1.6	-2.06	-6.88	13.20	6.1	1.16	1.10	3.60
B04	6.3	1.22	2.57	2.30					-2.1	-0.81	-3.14	30.60
B05					-2.8	0.78	-4.07	3.00	1.3	2.46	6.77	8.70
B06	0.6	1.00	25.50	0.00					-3.6	0.84	-2.36	6.40
B10									9.2	1.00	0.76	0.00
B11					-1.3	0.46	-9.08	2.40	13.4	1.00	0.63	0.00
B13	3.5	1.17	3.66	1.10	4.6	1.07	1.89	0.80	-2.2	0.68	-4.14	4.40
B14	6.9	1.00	0.59	0.00	-3.5	0.10	-3.71	12.80	4.1	1.07	1.64	1.00
B16	2.9	1.41	5.03	2.20	-3.6	0.64	-3.33	3.60	-3.7	0.35	-2.05	24.00
B18					-3.7	0.97	-3.30	0.30	-3.8	0.58	-2.29	6.30
B19	-2.0	0.60	-5.80	1.90					-3.1	0.97	-2.94	0.60
B20									3.6	1.19	2.11	3.10
B21									4.0	1.18	2.30	2.60
B22					-4.7	0.91	-2.57	1.60	10.8	1.06	0.83	1.20
B23	-3.2	0.87	-4.16	0.90	-3.1	1.00	-4.00	0.00	-4.0	0.90	-3.05	2.70
B25	-1.2	1.00	-9.25	1.80	-3.9	0.11	-3.23	8.90	-2.9	0.97	-3.17	0.60
B26	2.7	1.33	5.07	1.70					-4.3	0.35	-1.81	22.10
B27									10.1	1.04	1.13	0.90
B28									6.6	1.14	1.20	3.70
B30									5.3	1.02	1.51	0.50
B31									3.8	1.21	3.05	3.40
B33					-0.3	-1.53	-41.25	2.30	2.7	1.44	3.07	5.70
B34	7.0	1.07	1.60	1.30					-1.8	0.61	-4.67	3.70
B37									6.1	1.20	1.36	4.20
B38									1.9	1.11	4.16	0.80
B41									4.7	1.11	1.62	1.30
B42					-4.5	0.76	-2.87	3.70	2.4	1.75	4.79	5.50
B44	-3.1	0.55	-4.52	3.60					-4.1	0.78	-2.00	9.80
B45									4.4	1.50	1.77	8.60
B47					0.8	2.02	9.64	4.80	5.4	1.17	1.44	3.40
B49					-4.5	0.76	-2.87	3.70	-0.4	-0.76	-18.81	4.70
B54	-1.8	0.56	-6.39	3.70					-3.0	0.93	-2.73	2.40
B56									1.2	1.17	6.92	1.20
B60									2.7	1.93	3.78	13.00

Table 3, Continued

Analyte	30 mM				40 mM			
	μz^{eff}	α	β	Rs	μz^{eff}	α	β	Rs
B02	5.2	1.25	1.25	5.20	4.8	1.27	1.25	5.70
B04	-3.0	-0.53	-2.23	39.50	-2.5	-0.52	-2.48	25.60
B05	1.1	2.45	5.18	9.80	0.8	2.63	10.75	7.50
B06	-3.5	0.85	-1.91	7.10	-3.1	0.86	-2.00	6.50
B10	8.8	1.02	6.60	0.60	8.2	1.01	0.72	0.60
B11	12.1	1.03	0.49	0.90	11.5	1.03	0.51	1.23
B13	-2.2	0.64	-2.77	7.90	-2.2	0.64	-2.68	8.70
B14	3.6	1.08	2.00	1.40	3.5	1.09	1.60	2.10
B16	-3.6	0.39	-1.72	22.50	-3.5	0.37	-1.89	22.60
B18	-3.6	0.53	-1.72	8.00	-3.3	0.52	-2.03	7.20
B19	-2.8	0.96	-2.57	1.20	-2.8	0.96	-1.96	2.10
B20	2.7	1.26	2.67	3.00	2.2	1.27	2.73	3.30
B21	3.6	1.17	2.00	3.20	3.3	1.18	1.79	6.60
B22	9.5	1.05	0.77	1.70	9.3	1.06	0.65	2.10
B23	-3.7	0.95	-1.70	3.60	-3.6	0.92	-2.53	2.00
B25	-2.6	0.97	-2.35	1.20	-2.5	0.96	-2.44	1.00
B26	-3.7	0.38	-1.76	23.00	-3.3	0.39	-1.70	30.90
B27	9.1	1.04	0.71	1.80	8.5	1.05	0.72	1.60
B28	6.2	1.13	1.05	3.20	5.8	1.12	1.05	3.20
B30	4.8	1.02	1.38	0.50	4.4	1.02	1.34	0.70
B31	3.4	1.29	1.97	4.60	3.1	1.35	1.97	5.80
B33	2.6	1.42	2.58	5.40	2.4	1.42	1.21	10.00
B34	-1.8	0.72	-3.78	3.20	-1.6	0.69	-5.75	4.90
B37	5.5	1.25	1.02	5.70	5.4	1.26	1.11	6.90
B38	1.8	1.11	3.17	1.30	1.7	1.06	1.88	1.00
B41	4.2	1.19	1.40	2.50	3.9	1.18	1.54	3.00
B42	1.8	2.06	3.33	12.50	1.8	2.00	3.33	11.70
B44	-3.4	0.79	-1.79	9.70	-3.2	0.78	-1.91	8.20
B45	4.3	1.47	1.47	12.20	4.2	1.40	0.79	12.80
B47	5.1	1.20	1.59	3.10	4.9	1.18	0.71	4.60
B49	-0.9	0.23	-7.39	3.40	-0.9	0.49	-5.27	5.40
B54	-2.7	0.93	-2.44	2.50	-2.1	0.90	-2.86	1.90
B56	1.2	1.17	5.58	1.20	1.3	1.15	4.31	1.60
B60	2.3	2.13	3.43	10.70	2.2	2.00	1.23	24.20

baseline resolved. Another, more dramatic observation, is that, several of the analytes whose mobilities were measured in both acidic aqueous and acidic methanolic BGE's have a considerably more anionic mobility in the methanolic BGE than the same enantiomer whose mobility was measured in low pH aqueous BGE. This is the exact opposite trend observed for similar measurements using either HDMS, HDAS or ODAS.

3.5 Summary

A new, single-isomer, charged chiral resolving agent, ODMS, has been effectively used for the CE separation of the enantiomers of a large number of weak acids and weak bases in both low and high pH aqueous BGE's as well as for the separation of weak bases in an acidic methanolic BGE. The enantioselectivity afforded by ODMS appears unique among other SiSCD's as it presents a combined hydrophobic/ hydrophilic chiral environment for enantiorecognition. ODMS had a limited utility for the separation of non-ionic enantiomers.

CHAPTER IV

CONCLUSIONS

The synthetic methodology used to produce ODMS utilized protection group chemistry to allow regioselective per-modification of the secondary hydroxyl groups. Subsequent steps included deprotection followed by complete sulfation of the primary hydroxyl groups. Thorough analytical characterization of ODMS and each of its synthetic intermediates was accomplished using HPLC-ELSD, indirect UV-detection CE, 1-D and 2D ^1H and ^{13}C -NMR, MALDI-TOF mass spectrometry and X-ray crystallography. These characterization methods, when interpreted together, yielded convincing evidence that ODMS is isomerically pure and has the expected substitution pattern.

Use of ODMS for the separation of weakly basic enantiomers in pH 2.5 aqueous BGE's showed that most exhibit one of two specific mobility trends; those that are strongly binding and thus, have anionic mobilities at very low ODMS concentrations and those that are weakly binding with only moderate change in their cationic effective mobility. Since most analytes showed only weak binding, ODMS offers the potential for resolution of enantiomers with very short analysis times. Also, for both weakly basic and weakly acidic enantiomers, weak binding characteristics typical to ODMS resulted in good resolution of the analytes due to improved β values. High pH measurements were not as successful. Poor β values resulted in low resolution separations even when separation selectivity values were the same or comparable to those observed in the low

pH BGE. However, it was shown that, at least for the weakly basic and weakly acidic analytes, a high pH BGE can offer different separation selectivity patterns from that observed in low pH BGE's which may prove to be invaluable in the analysis of more complex enantiomer mixtures.

Even more successful was the use of ODMS for enantiomer separations in an acidic methanolic BGE where higher potentials and good β values resulted in very fast analysis times. Often, baseline resolution was observed in under 5 minutes with very low ODMS concentrations. ODMS was found to be a more versatile chiral resolving agent when used in acidic methanolic BGE's than in aqueous BGE's as a third mobility trend, for moderately binding analytes, was observed. While these are important findings, probably the most surprising result was that many enantiomers separated both in acidic aqueous and acidic methanolic BGE's showed increased binding strengths in the acidic methanolic BGE. This was unexpected both due to previous work with other SiSCD's where the opposite trend was more common and because of a preconceived notion that methanol would act as a stronger competing agent resulting in reduced complexation constants than observed in an aqueous BGE. While the number of separations that can be compared using both BGE's with an SiSCD other than ODMS is limited, the change in the mobility trends means that greater control can be exerted over the mobility of an analyte. Again, this knowledge may prove invaluable for the separation of more complex mixtures.

In conclusion, a novel, single-isomer, sulfated cyclodextrin, the sodium salt of octakis(2,3-di-O-methyl-6-O-sulfo) cyclomaltooctaose (ODMS), has been produced on

the large scale with greater than 98% isomeric purity. It has been successfully used as a chiral resolving for capillary electrophoretic separation of weakly acidic and weakly basic enantiomers in aqueous and methanolic BGE's and with limited success for the resolution of non-ionic enantiomers. ODMS has been shown to offer unique mobility and separation selectivity trends as compared to other single-isomer, sulfated CD's.

REFERENCES

- [1] US Food and Drug Administration Policy Announcement, *Chirality* 4 (1992) 338.
- [2] Y. Berezinski, R. Thompson, E. O'Neill, N. Grinberg, *J. of AOAC Int.* 84 (2001) 1242.
- [3] V. Schurig, *J. Chromatogr. A* 906 (2001) 275.
- [4] H. Soon, *Biomedical Chromatogr.* 11 (1997) 259.
- [5] Y. Tanaka, S. Terabe, *J. Biochem. and Biophys. Methods* 48 (2001) 103.
- [6] K. Otsuka, S. Terabe, *J. Chromatogr. A* 875 (2000) 163.
- [7] Y. Deng, J. Henion, J. Li, P. Thibeault, C. Wang, D.J. Harrison, *Anal. Chem.* 73 (2001) 639.
- [8] T. Liu, J. Li, R. Zeng, X. Shao, K. Wang, Q. Xia, *Anal. Chem.* 73 (2001) 5875.
- [9] A. I. Gusev, *Fresenius' J. Anal. Chem.* 366 (2000) 691.
- [10] S. A. Korhammer, A. Benreuther, *Fresenius' J. Anal. Chem.* 354 (1996) 131.
- [11] S. McWhorter, S. Soper, *Electrophoresis* 21 (2000) 1267.
- [12] A. D. Sokolowski, Gy. Vigh, *Electrophoresis* 22 (2001) 3824.
- [13] R. F. Cross, J. Cao, *J. Chromatogr. A* 786 (1997) 171.
- [14] M. F. M. Tavares, V. L. McGuffin, *Anal. Chem.* 67 (1995) 3687.
- [15] Y. Y. Rawjee, Gy. Vigh, *Anal. Chem.* 66 (1994) 428.
- [16] R. Kuhn, *Electrophoresis* 20 (1999) 2605.
- [17] C. Garcia, Y. Pointud, G. Jeminet, D. Dugat, *Tet. Let.* 40 (1999) 4993.
- [18] A. Rizzi, *Electrophoresis* 22 (2001) 3079.

- [19] Gy. Vigh, A. Sokolowski, *Electrophoresis* 18 (1997) 2305.
- [20] H. Nishi, S. Terabe, *J. Chromatogr. A* 694 (1995) 245.
- [21] S. Fanali, *J. Chromatogr. A* 875 (2000) 89.
- [22] G. Gubitz, M. Schmid, *Electrophoresis* 21 (2000) 4112.
- [23] G. Wenz, *Angew. Chem. Int. Ed. Engl.* 33 (1994) 803.
- [24] P. Andrighetto, T. Carofiglio, R. Fornasier, U. Tonellato, *Electrophoresis* 21 (2000) 619.
- [25] X. Zhu, B. Lin, A. Jakob, S. Wuerthner, B. Koppenhoefer, *Electrophoresis* 20 (1999) 1878.
- [26] M. L. Bender, *Cyclodextrin Chemistry*, Springer-Verlag, Berlin, 1977.
- [27] H. Schneider, F. Hacket, V. Rudiger, *Chem. Rev.* 98 (1998) 1755.
- [28] F. Hirayama, S. Mieda, Y. Miyamoto, H. Arima, K. Uekama, *J. Pharm. Sci.* 88 (1999) 970.
- [29] M. Nielen, *Anal. Chem.* 65 (1993) 885.
- [30] O. Zerbini, F. Trotta, C. Giovannoli, C. Baggiani, G. Giraudi, A. Vanni, *J. Chromatogr. A* 810 (1998) 193.
- [31] S. Izumoto, H. Nishi, *Electrophoresis* 20 (1999) 189.
- [32] H. Cai, Gy. Vigh, *J. Microcol. Sep.* 10 (1998) 293.
- [33] W. Zhu, W. Li, F. Raushel, Gy. Vigh, *Electrophoresis* 21 (2000) 3249.
- [34] S. Sabah, G. Scriba, *J. Chromatogr. A* 833 (1999) 261.
- [35] Y. J. Heo, Y. S. Whang, M. K. In, K. Lee, *J. Chromatogr. B* (2000) 221.
- [36] F. Wang, M. Khaledi, *Electrophoresis* 19 (1998) 2095.

- [37] G. Schulte, B. Chankvetadze, G. Blaschke, *J. Chromatogr. A* 771 (1997) 259.
- [38] R. J. Tait, D. O. Thompson, V. J. Stella, J. F. Stobaugh, *Anal. Chem.* 66 (1994) 4013.
- [39] B. Chankvetadze, G. Endresz, G. Blaschke, *Electrophoresis* 15 (1994) 804.
- [40] F. O'Keefe, S. Shamsi, R. Darcy, I. Warner, *Anal. Chem.* 69 (1997) 4773.
- [41] T. Schmitt, H. Engelhardt, *Chromatographia* 37 (1997) 475.
- [42] J. Szeman, K. Ganzler, A. Salgo, J. Szejtli, *J. Chromatogr. A* 728 (1996) 423.
- [43] E. Francotte, L. Brandel, M. Jung, *J. Chromatogr. A* 792 (1997) 379.
- [44] Y. Y. Rawjee, D. U. Staerk, *Gy. Vigh, J. Chromatogr. A* 635 (1993) 291.
- [45] Y. Y. Rawjee, R. Williams, *Gy. Vigh, J. Chromatogr. A* 652 (1993) 233.
- [46] Y. Y. Rawjee, R. Williams, *Gy. Vigh, J. Chromatogr. A* 680 (1994) 599.
- [47] B. A. Williams, *Gy. Vigh, J. Chromatogr. A* 777 (1997) 295.
- [48] J. B. Vincent, *Gy. Vigh, J. Chromatogr. A* 817 (1998) 105.
- [49] D. K. Maynard, *Gy. Vigh, Electrophoresis* 22 (2001) 3152.
- [50] W. Zhu, *Gy. Vigh, J. Micro. Col. Sep.* 12 (2000) 167.
- [51] W. Zhu, *Gy. Vigh, J., Chromatogr. A* 895 (2000) 247.
- [52] W. Zhu, *Gy. Vigh, J. Chromatogr. A* 892 (2000) 299.
- [53] J. B. Vincent, *Gy. Vigh, J. Chromatogr. A* 816 (1998) 233.
- [54] M. Tacker, P. Glukhovskiy, H. Cai, *Gy. Vigh, Electrophoresis* 20 (1994) 2794.
- [55] W. Zhu, *Gy. Vigh, Electrophoresis* 21 (2016).
- [56] H. Cai, *Gy. Vigh, J. Chromatogr. A* 827 (1998) 121.
- [57] J. B. Vincent, A. D. Sokolowski, T. V. Nguyen, *Gy. Vigh, Anal. Chem.* 69 (1997)

4226.

- [58] H. Cai, T. V. Nguyen, Gy. Vigh, *Anal. Chem.* 70 (1998) 580.
- [59] J. B. Vincent, D. M. Kirby, T. V. Nguyen, Gy. Vigh, *Anal. Chem.* 69 (1997) 4419.
- [60] W. Zhu, Gy. Vigh, *Anal. Chem.* 72 (2000) 310.
- [61] W. Zhu, Gy. Vigh, *Electrophoresis* 22 (2001) 1394.
- [62] A. R. Khan, P. Forgo, K. J. Stine, V. T. D'Souza, *Chem. Rev.* 98 (1998) 1977.
- [63] P. S. Bansal, C. L. Francis, N. K. Hart, S. A. Harrison, D. Oakenfull, A. D. Robertson, G. W. Simpson, *Aust. J. Chem.* 51 (1998) 915.
- [64] A. P. Croft, R. A. Bartsch, *Tetrahedron* 39 (1983) 1417.
- [65] D. Klemm, A. Stein, U. Erler, W. Wagenknecht, I. Nehls, B. Philipp, *Cellulose*, Ellis Horwood, Chichester, 1993.
- [66] P. Mischnick, M. Lange, M. Gohdes, A. Stein, K. Petzold, *Carbohydrate Res.* 277 (1995) 179.
- [67] D. Icheln, B. Gercke, Y. Piprek, P. Mischnick, W. A. König, M. A. Dessoy, A. F. Morel, *Carbohydrate Res.* 280 (1996) 237.
- [68] W. K. Russell, D. H. Russell, M. B. Busby, A. Kolberg, S. Li, D. K. Maynard, S. Sanchez-Vindas, W. Zhu, Gy. Vigh, *Carbohydrate Res.* 287 (2001) 325.
- [69] K. Takeo, H. Mitoh, K. Uemura, *Carbohydrate Res.* 187 (1989) 203.
- [70] B. A. Williams, Gy. Vigh, *Anal. Chem.* 69 (1997) 4445.

APPENDIX A
LETTERS OF COPYRIGHT CREDIT



Our ref: HW/NIC/June02-350

B Busby
Texas A & M University
Department of Chemistry
PO Box 30012
College Station
TX 77842-3012
USA
Fax: 979 845 4719

Dear Dr Busby

JOURNAL OF CHROMATOGRAPHY A, Vol 914, Issue 1, 2001, pp 325-330, Russell et al. "Artifact-free matrix assisted laser. . .", table 1 & conclusions

As per your letter dated 30 May 2002, we hereby grant you permission to reprint the aforementioned material at no charge in your thesis subject to the following conditions:

1. If any part of the material to be used (for example, figures) has appeared in our publication with credit or acknowledgement to another source, permission must also be sought from that source. If such permission is not obtained then that material may not be included in your publication/copies.
2. Suitable acknowledgment to the source must be made, either as a footnote or in a reference list at the end of your publication, as follows:
"Reprinted from Publication title, Vol number, Author(s), Title of article, Pages No., Copyright (Year), with permission from Elsevier Science".
3. Reproduction of this material is confined to the purpose for which permission is hereby given.
4. This permission is granted for non-exclusive world **English** rights only. For other languages please reapply separately for each one required. Permission excludes use in an electronic form. Should you have a specific electronic project in mind please reapply for permission.
5. This includes permission for UMI to supply single copies, on demand, of the complete thesis. Should your thesis be published commercially, please reapply for permission.

Yours sincerely



Frances Rowwell
Global Rights Manager

Your future requests will be handled more quickly if you complete the online form at www.elsevier.com

Elsevier Science, Global Rights Department, PO Box 800, Oxford OX5 1DX, UK
Tel +44 (0)1865 843830 | Fax +44 (0)1865 853333 | www.elsevier.com
vat no. 494 6272 12

Academic Press • Butterworth-Heinemann • Cell Press • Churchill Livingstone • Engineering Information • Excerpta Medica
Fluka • Harwood Academic • Intech • MDPI • Mosby • North-Holland • Persamon • ScienceDirect • WB Saunders
TOTAL P. 01

Dear Ms. Rutz,

Thank you for granting me copyright permission to include this work in my thesis. Due credit will be given to the original source at the head of each chapter referencing the copyrighted material.

Is it possible to receive a hard copy to be included in the thesis granting permission, preferably with a company letterhead? I have included a

fax number you can use if you desire. If not, please, contact me for some other more appropriate means for sending the hard copy. Thank you for your assistance in this matter.

Sincerely,
M. Brent Busby
Fax# 979-845-4719

----- Original Message -----
From: "Claudia Rutz" <CRutz@wiley-vch.de>
To: "Brent Busby" <busby@mail.chem.tamu.edu>
Sent: Friday, May 31, 2002 2:01 AM
Subject: Antwort: copyright permission

Dear Mr. Busby,

Thank you for your e-mail from today.

We hereby grant permission for the requested use. We expect that due credit will be given to the original source.

With kind regards

Sincerely yours,

Claudia Rutz
.....
Claudia Rutz
Copyright/Licensing Manager
WILEY-VCH Verlag GmbH
Bonchstraße 12
D-69469 Weinheim
Germany
Phone: +49 6201 606 280
Fax: +49 6201 606 332
email: CRutz@wiley-vch.de

We hereby grant permission for the requested use expected that due credit is given to the original source.

WILEY-VCH, STM-Copyright & Licenses

C. Rutz

Weinheim, June 6, 2002

"Brent Busby"
<busby@mail.chem.tamu.edu>

An: <crutz@wiley-vch.de>
Kopia:
Theme: copyright permission

31.05.2013 00:04

Dear Ms. Rutz,

I am a master's degree candidate at Texas A&M University and will be finalizing my thesis within the next two months. My reason for writing is to request permission to use information from a manuscript I have published in your journal. I will be using part of the tabular information included in the article that I co-authored with Omar Maldonado and Cynthia Vigh. This article appeared on pp. 456-461 of issue 23 of your journal. The title is Nonaqueous capillary electrophoretic separation of enantiomers using

APPENDIX B
EXPERIMENTAL

Octakis(6-O-t-butyltrimethylsilyl)cyclomaltooctaose (2).— To a mechanically stirred, sealed reaction vessel containing a solution of dry **(1)** (1.8 kg), imidazole (0.79 kg) and DMAP (0.03 kg) in dry DMF (2.6 L), add dropwise over a one week period a solution of TBDMSCl (0.84 kg) in EtOAc (1.68 L) followed by dropwise addition over a one week period of a solution of TBDMSCl (0.84 kg) in EtOAc (2.52 L). Add imidazole (0.05 kg) to the DMF/EtOAc mixture and add dropwise over a one day period a solution of TBDMSCl (104.5 g) in EtOAc (0.31 L). Repeat this last step until the undersilylated side-product is lower than 1% as measured by RP HPLC-ELSD (MeOH-EtOAc). Add EtOAc (4 L) and filter the imidazolium chloride on a Buchner funnel. Add EtOAc (4 L) to the filtrate and stir 12 hr to precipitate the crude product. Filter the crude product on a Buchner funnel and wash with water (3 × 2 L). Digest the washed, crude product in refluxing acetone (14 L) to obtain **(1)** as white powder until over-silylated material is less than 0.1 area % of the target peak as measured by RP HPLC-ELSD. Recrystallize the white powder from methanol (2-3 × 9 L) until the under-silylated side-product is less than 0.3 area % of the target peak as measured by RP HPLC-ELSD and dry in vacuo at 110 °C to a constant mass to yield **(2)** (2.05 kg, 67%).

Octakis(2,3-di-O-methyl-6-O-sulfo)cyclomaltooctaose (3).— To a mechanically stirred, sealed reaction vessel containing a mixture of dry NaH (87 g, 60% dispersion in mineral oil) in THF (3.75 L) add over a 40 min time period a solution of **(2)** (250 g) and CH₃I (169 mL) in THF (1 L) and stir for 5 hr while monitoring for completion by RP HPLC-ELSD (MeOH:EtOAc). Add MeOH (50 mL) to quench. Add BuOAc (1.3 L) and evaporate to dryness. Filter the NaI precipitate on a Buchner funnel prior to precipitation

of crude product. To the crude material add water (3×1 L) and evaporate to dryness. Add anhydrous ethanol (3×2 L) and evaporate to dryness. Dry in vacuo at $60\text{ }^{\circ}\text{C}$ overnight to obtain **(3)** as a bright yellow powder (307 g, 97%).

Octakis(2,3-di-O-methyl)cyclomaltooctaose (4).— To a magnetically stirred solution of **(3)** (400g) in anhydrous EtOH (2 L), slowly add HF (334 mL, 48% aq. soln.). Continue stirring for 12 hr. Monitor completion of the reaction by NP HPLC-ELSD (MeOH: EtOAc). Place the reaction vessel in an ice bath and add dropwise over a 1 hr period a solution of NaOH (350 g) in water:anhydrous ethanol (0.3:1.44 L) to a phenolphthalein endpoint. Evaporate to dryness and filter the NaI precipitate on a Buchner funnel prior to precipitation of the crude product. Recrystallize in acetone ($5\text{-}6 \times 3$ L) to obtain **(4)** (99% pure by HPLC) as a white powder (181 g, 72%).

Octakis(2,3-di-O-methyl-6-O-sulfo)cyclomaltooctaose (5).— To a magnetically stirred solution containing **(4)** (250 g) in DMF (375 mL) add Pyr-SO₃ complex (251 g). Continue stirring for 2 hr and pour into acetone (3.75 L). Decant and dissolve the amorphous solid in 6.6 M NaOH (240 mL). Add anhydrous EtOH (3 L) and evaporate to dryness. Precipitate the crude material from solution in a minimum volume of water made basic with 10 M NaOH and $6 \times$ water volume of anhydrous ethanol. Repeat until isomeric purity is acceptable and no dimethylamine peaks are observed in the ¹H-NMR. Filter on a Buchner funnel the material from 50 mM solution in MeOH to remove Na₂SO₄. Evaporate to dryness from water (5 L) to obtain **(5)** as a white solid.

VITA

Brent Busby graduated from Robert E. Lee high school, Tyler, TX in 1991. He attended Tyler Junior College, Tyler, TX from 1991-1995 and graduated May 1995 with an Associate of Science in chemistry. He attended the University of Texas at Tyler, Tyler, TX from 1995-1998 and graduated with a Bachelor of Science in Chemistry. He attended Texas A&M University, College Station, TX from 1998-2002 and graduated with a Master of Science in chemistry under the direction of Professor Gyula Vigh in August, 2002. He can be reached at Texas A&M University, Department of Chemistry, P.O. Box 3012, College Station, TX, 77843-3012.